New Atmospheric Muon Physics Results with the MINOS Far Detector

Brian Rebel

August 2007

Outline

- Cosmic ray muons and atmospheric neutrinos
- Introduction to MINOS
- Event selection
- Neutrino-induced muon results: PRD 75:092003 (2007)
- Cosmic ray charge ratio: hep-ex/0705.3815 (accepted by PRD
- Note - Atmospheric neutrino contained vertex analysis previously presented: PRD 73:072002 (2006)

Cosmic Ray Muons and Atmospheric Neutrinos

- Cosmic ray muons produced by primaries interacting in upper atmosphere
- Pions and kaons produced in initial interactions, then decay into muons and neutrinos
- Similar decay chain to the NuMI beam
- However very different energy range
  - Cosmic ray primaries range 10^2 - 10^{11} GeV
  - Atmospheric neutrinos < 1 - 10^5 GeV

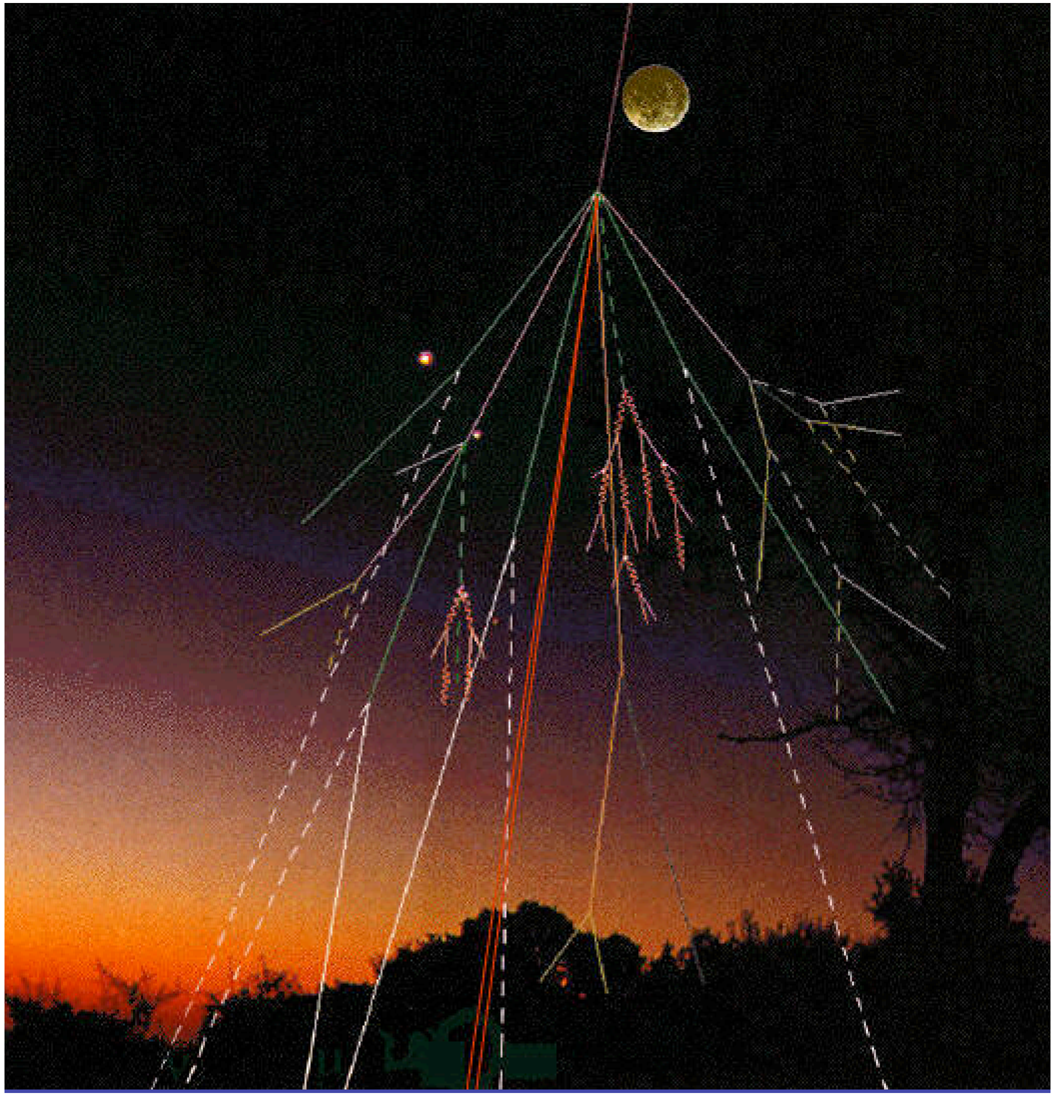

Muon and Neutrino Production

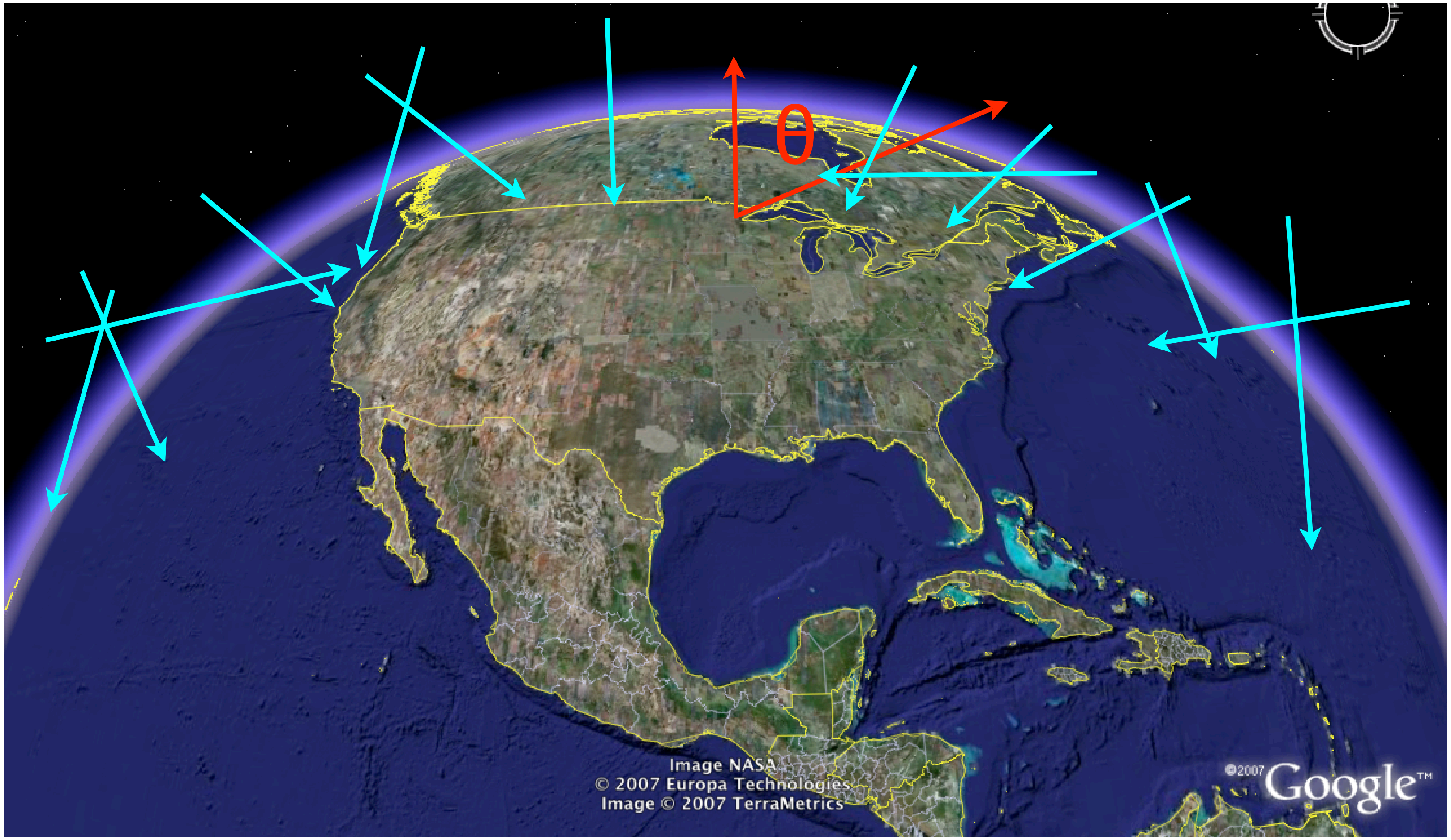

- Muons and neutrinos are produced isotropically
- Rate at surface depends on zenith angle and muon energy

$$\frac{dN_\mu}{dE_\mu} = \frac{0.14 E_\mu^{-2.7}}{cm^2 ssr GeV}\left(\frac{1}{1+\frac{1.1E_\mu \cos\theta}{115GeV}} + \frac{0.054}{1+\frac{1.1E_\mu \cos\theta}{850GeV}}\right)$$

T. Gaisser

Cosmic Ray Muons vs Neutrino-Induced Muons

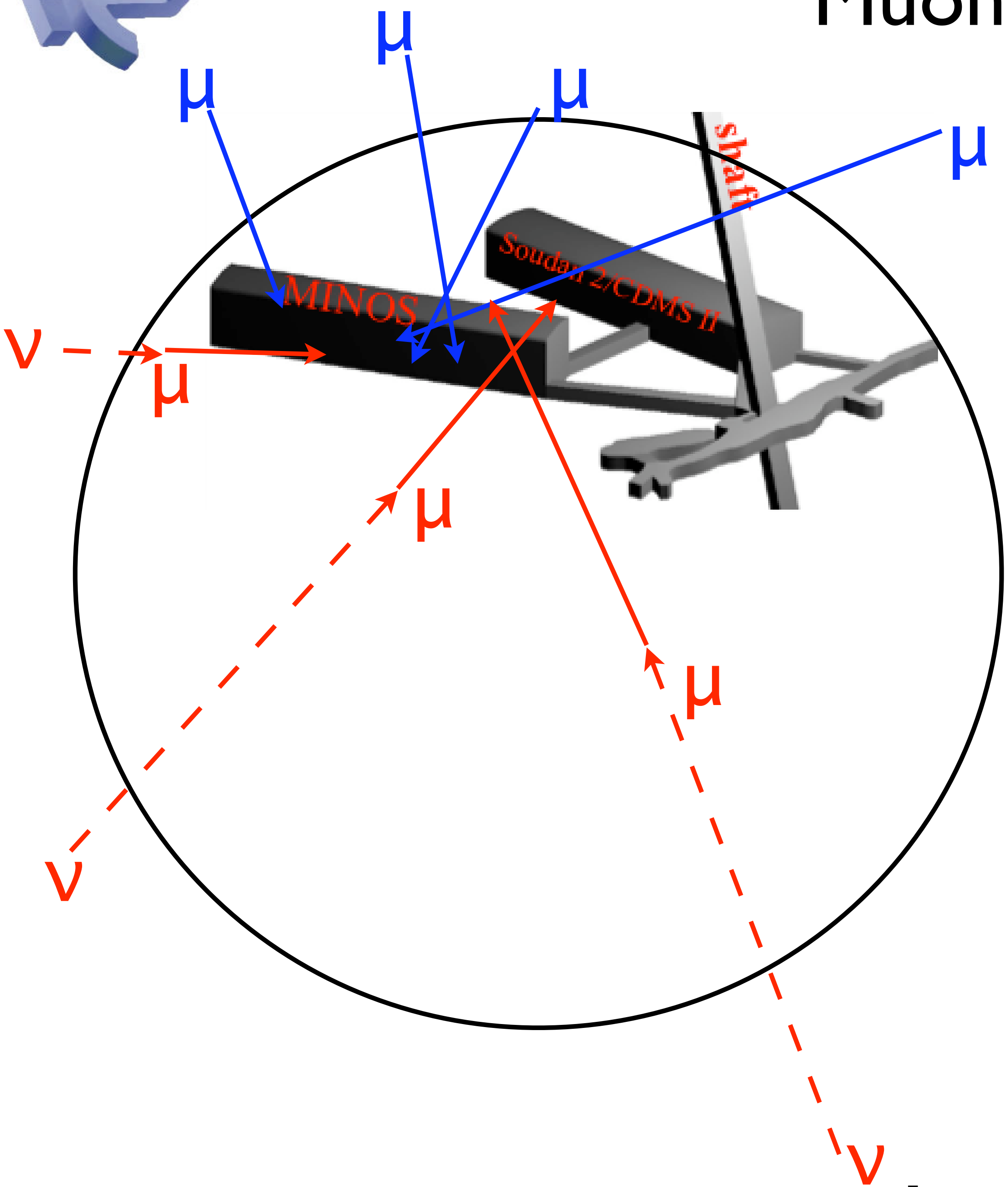

- Cosmic ray muons come down
- Rate underground determined by overburden of rock above detector
- Neutrino-induced muons from horizon and below
- Need a lot of rock to filter out highest energy cosmic ray muons $\sim 10^5$ g/cm^2
- Relative rate of cosmic ray muons to neutrino-induced muons 10^5:1

MINOS Overview

- Main Injector Neutrino Oscillation Search is a long baseline neutrino oscillation experiment
- Measure the neutrinos on site with the near detector
- Measure them again using far detector 735 km away in Soudan Mine
- MINOS main goal is to make a precision measurement of Δm^2_{32} (recent W&C talk)
- Will also look for sterile neutrinos, ν_e appearance in the beam
- Measurements on cosmic ray muons and atmospheric ν_μ and $\bar{\nu}_\mu$

MINOS Overview

- Main Injector Neutrino Oscillation Search is a long baseline neutrino oscillation experiment
- Measure the neutrinos on site with the near detector
- Measure them again using far detector 735 km away in Soudan Mine
- MINOS main goal is to make a precision measurement of Δm^2_{32} (recent W&C talk)
- Will also look for sterile neutrinos, ν_e appearance in the beam
- Measurements on cosmic ray muons and atmospheric ν_μ and $\bar{\nu}_\mu$

MINOS Far Detector

- Far Detector is located in Soudan Underground Mine - 2341 feet below the surface
- Far detector construction began August 2001, finished in July 2003
- First beam events January 2005
- Far detector collecting data for over 4 years

MINOS Far Detector

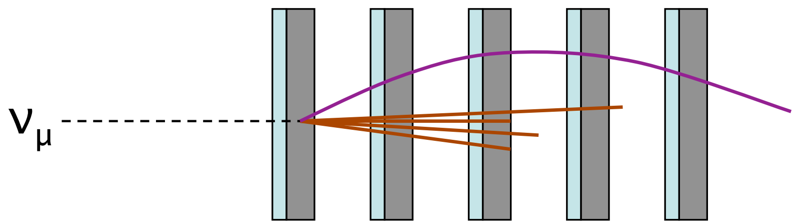

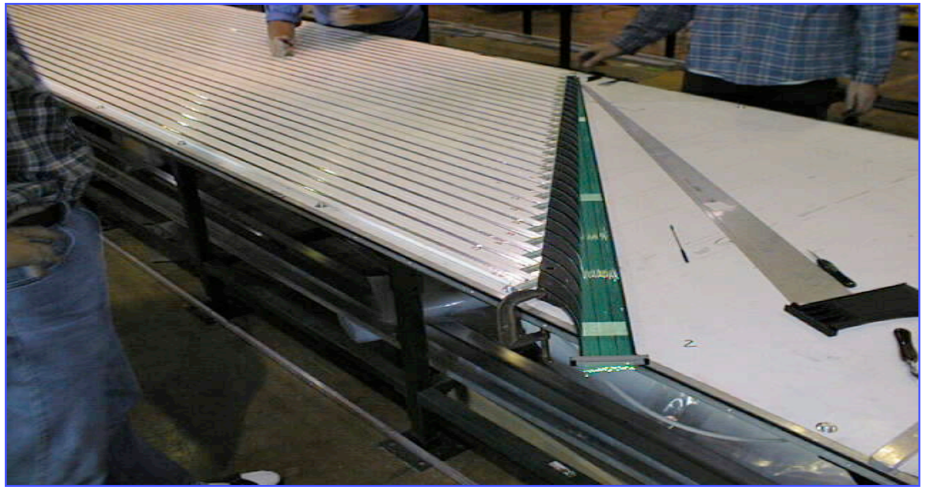

- Detector is made of alternating layers of 2.54 cm steel and 1 cm scintillator
- Strips of scintillator mounted to steel absorber
- Strips are 4.1 cm wide, up to 8 m long
- Wavelength-shifting (green) fiber used to collect scintillation light
- Clear fiber used to bring signal to photomultiplier tubes (PMTs)
- PMTs have pixels to read out signals from multiple strips

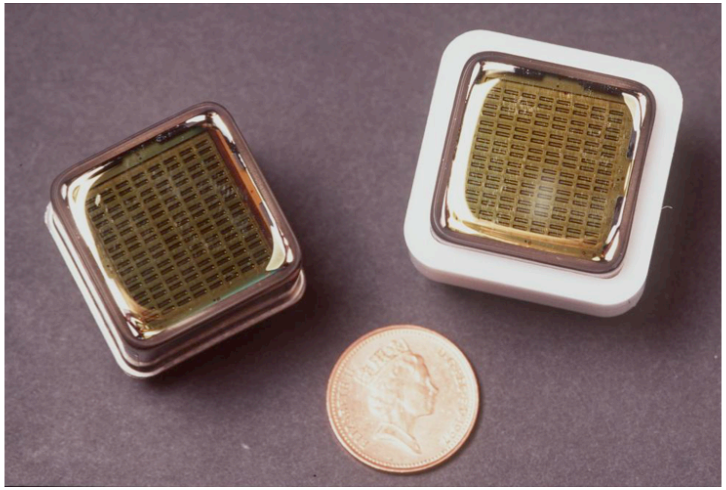

Far Detector

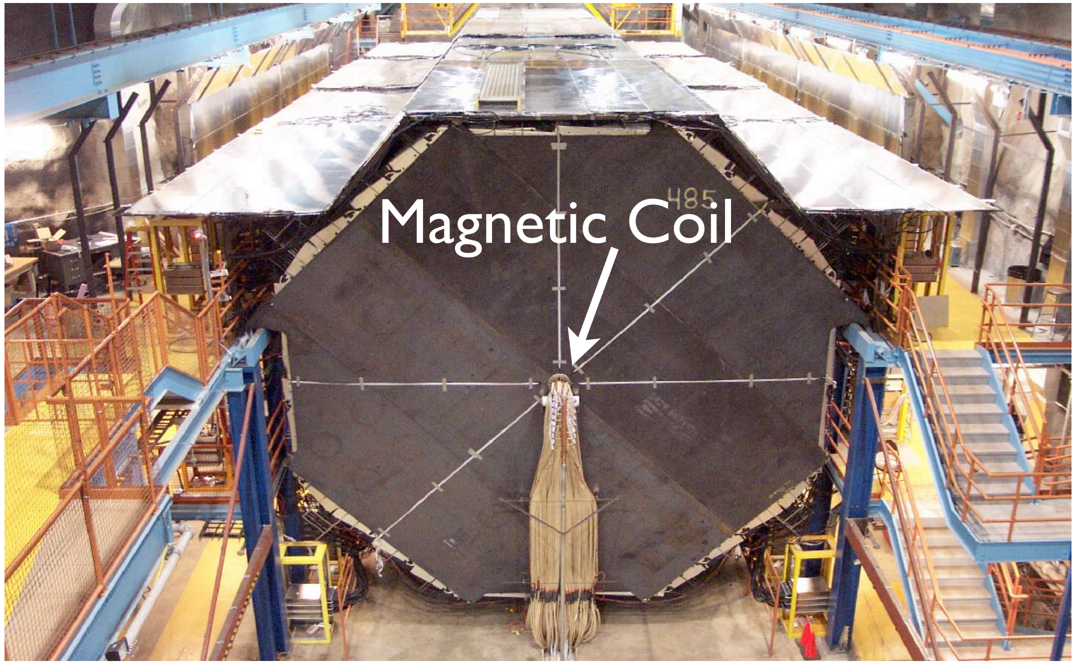

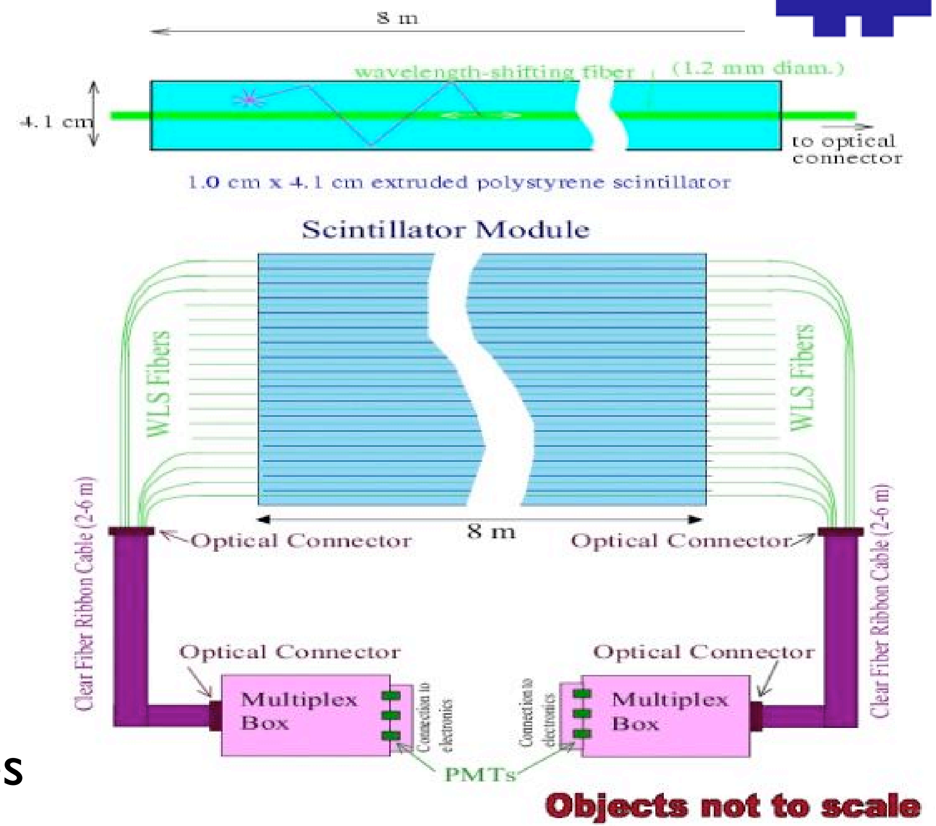

- 5.4 kT, 8 m octagon, 484 instrumented planes
- Double ended readout
- M16 PMTs
- Optical summing with 8 strips mapped to each PMT pixel
- Front end electronics capable of good timing resolution - important to select neutrino induced muons, beam neutrinos

Far Detector Magnetic Field

- MINOS is first magnetized large underground detector
- Toroidal magnetic field with average field strength 1.3 T
- Able to separate μ^- from μ^+ for large range of momenta: 1 - 250 GeV

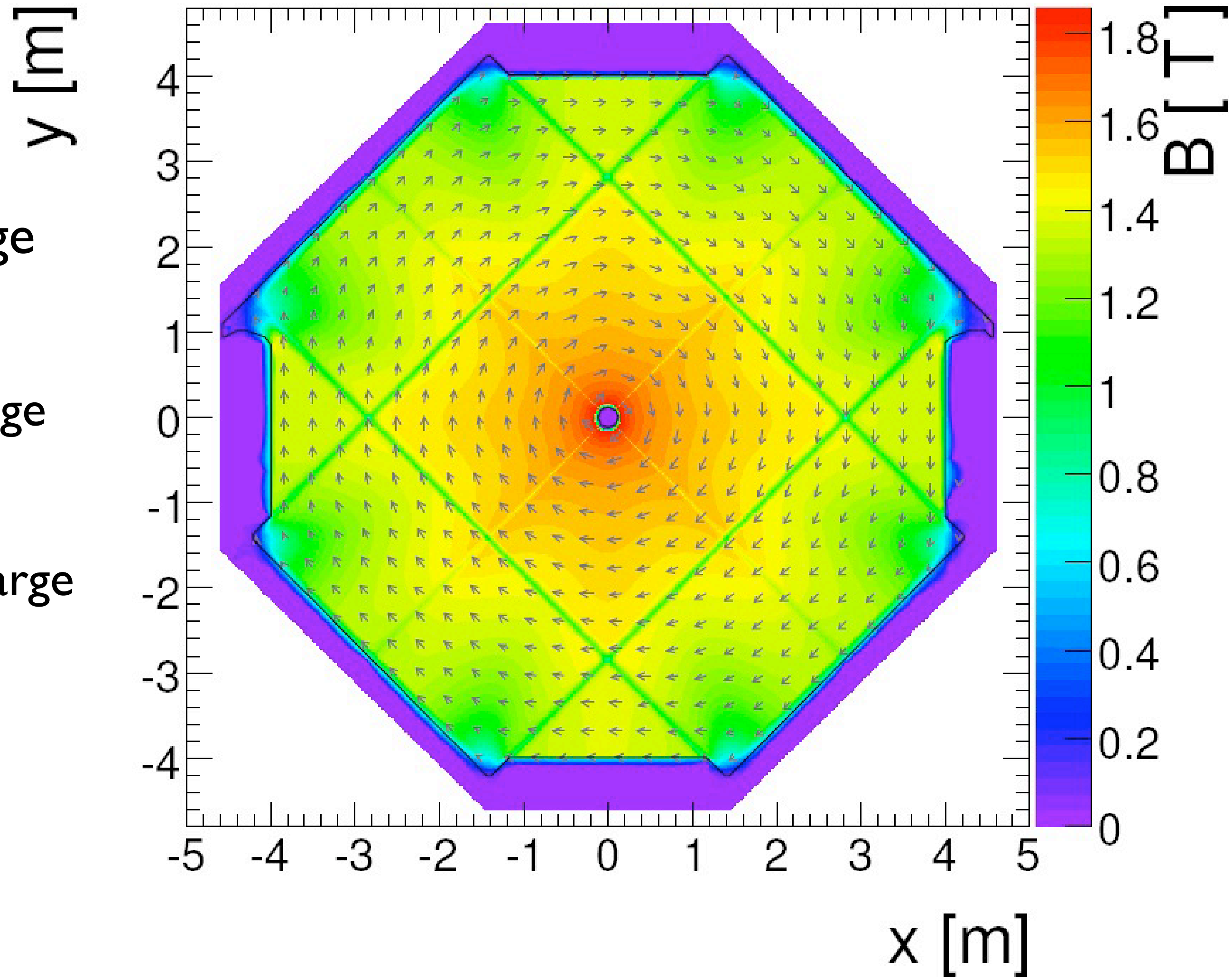

The MINOS Collaboration

Argonne - Athens - Benedictine - Brookhaven - Caltech - Cambridge - Campinas - Fermilab - College de France - Harvard - IIT - Indiana - Minnesota - Minnesota-Duluth - Oxford - Pittsburgh - Rutherford - Sao Paulo - South Carolina - Stanford - Sussex - Texas A&M - Texas - Tufts - University College London - William & Mary - Wisconsin

27 institutions, 175 scientists, funded by DOE, NSF, SFTC

Cosmic Ray Event Display

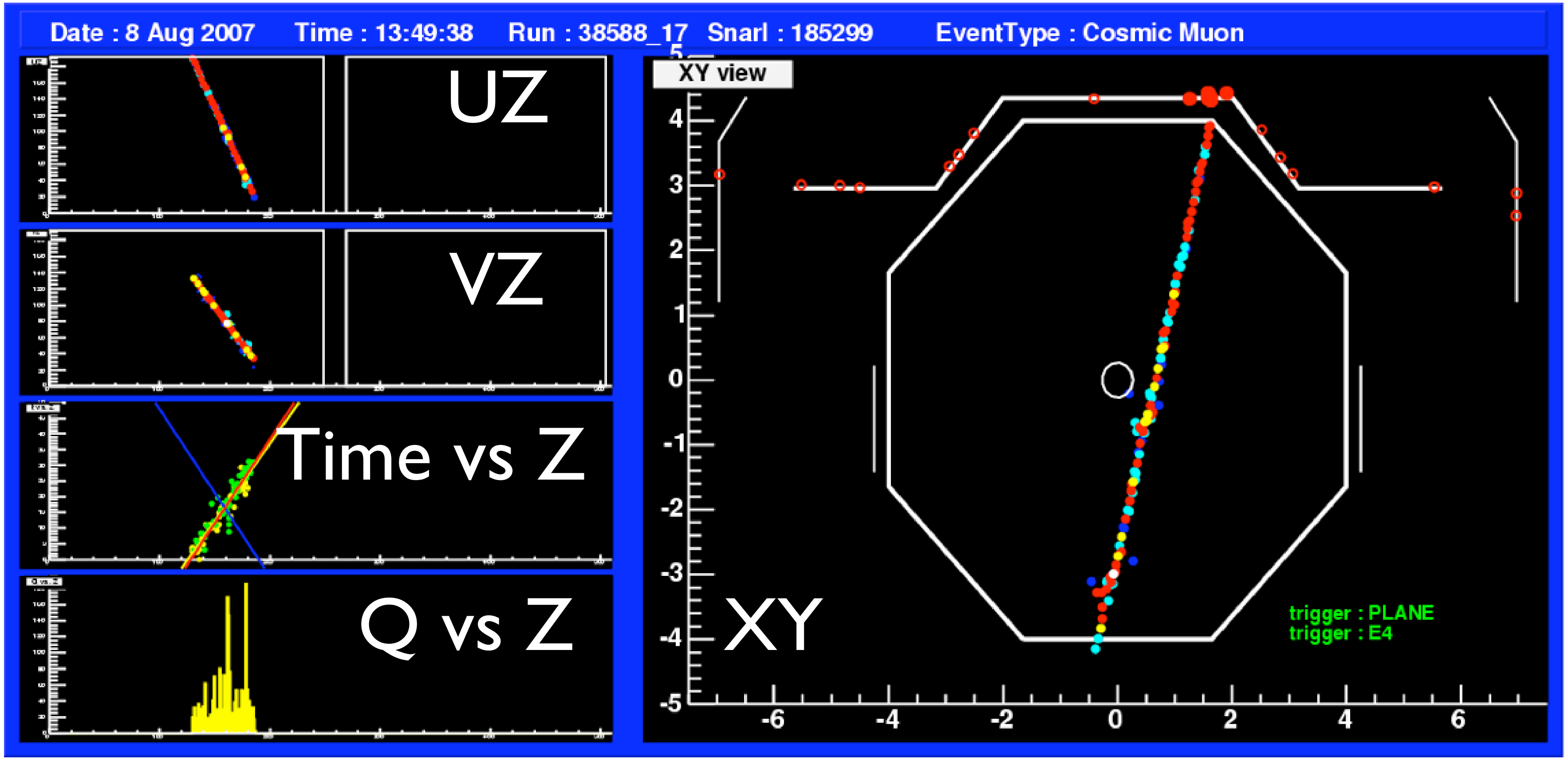

- Top left plots show UZ and VZ views
- Bottom left plots show time and charge vs Z
- Right plot is XY view
- Typical through going muon

Cosmic Ray - Multiple Muon Event

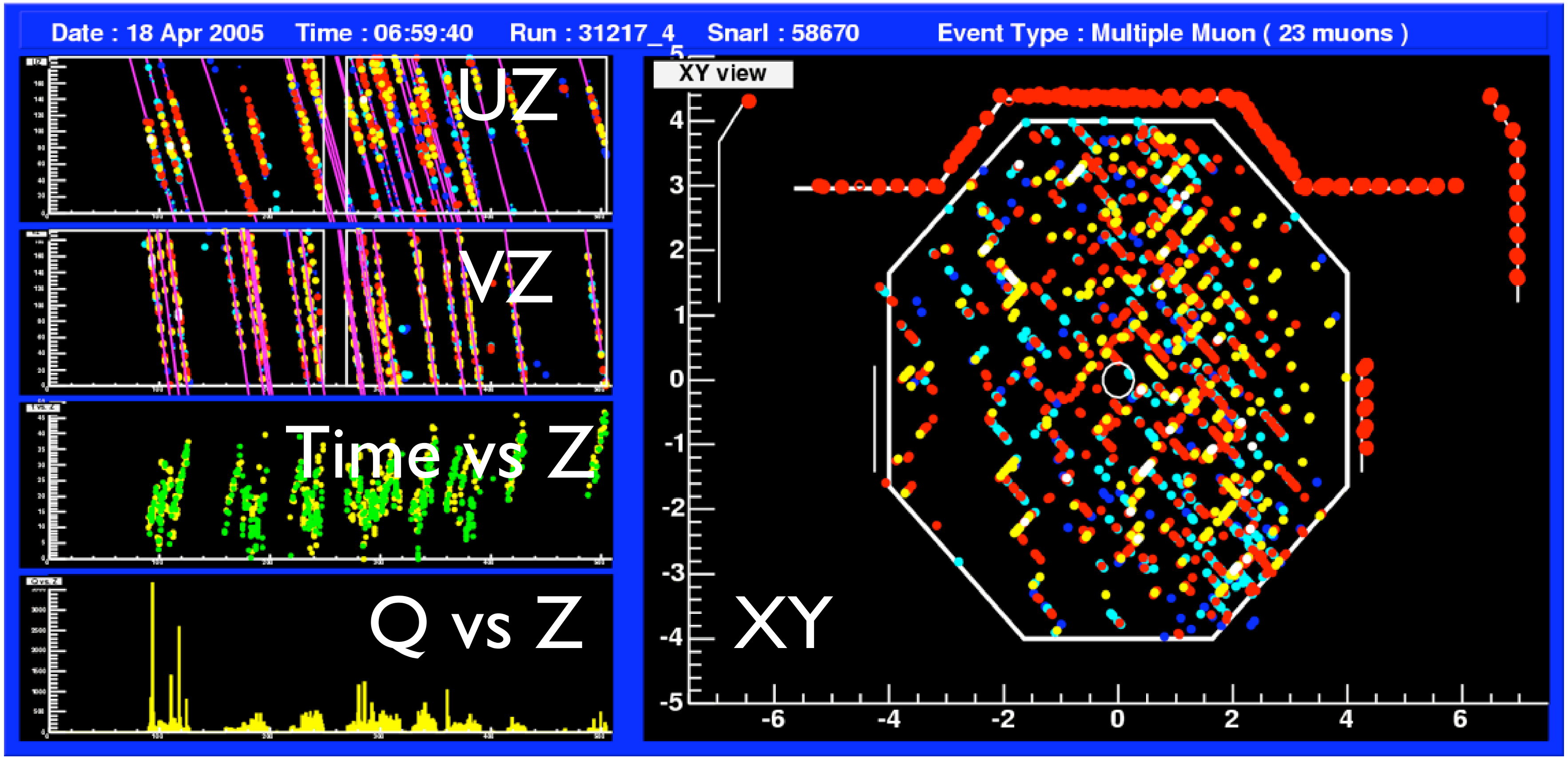

- ~4% of all muons are from multiple muon events
- Example of very high multiplicity
- These events are removed from the analysis

Muon Direction Determination

- Need to know how muon moves through detector
  - cosθ - where it came from
  - Charge determination
- Initial direction found by determining slope of T vs Z
- Need to cross several planes to have accurate slope
- Hit with smallest time is entrance point or vertex

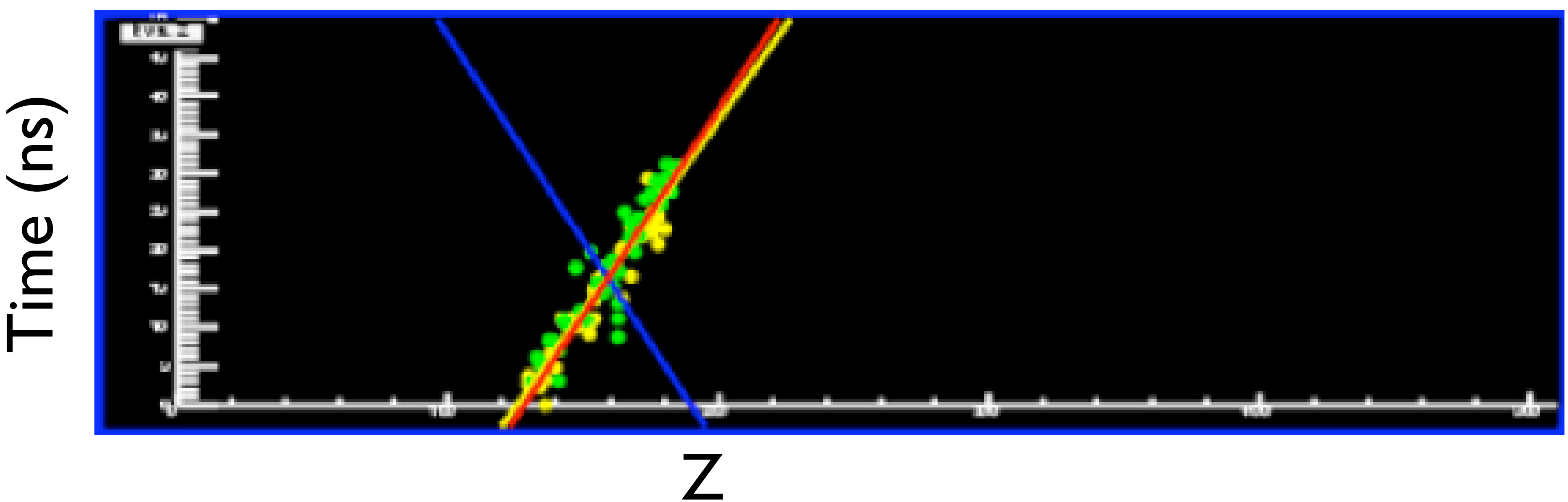

Event Selection

- Cosmic ray muons and atmospheric neutrino-induced muons leave similar tracks
- Many of selection requirements over lap
- Exclude multiple muons
- Fiducial cut - require muon to enter the detector
- Require good track in event
  - Cross enough planes for track finding/fitting
  - Long enough to get accurate timing
  - Good fit for charge and momentum determination

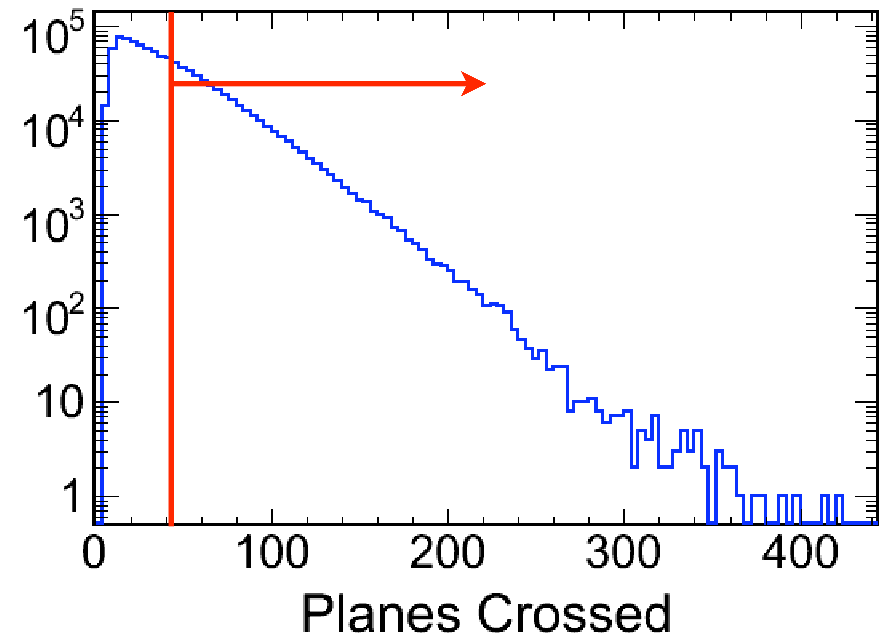

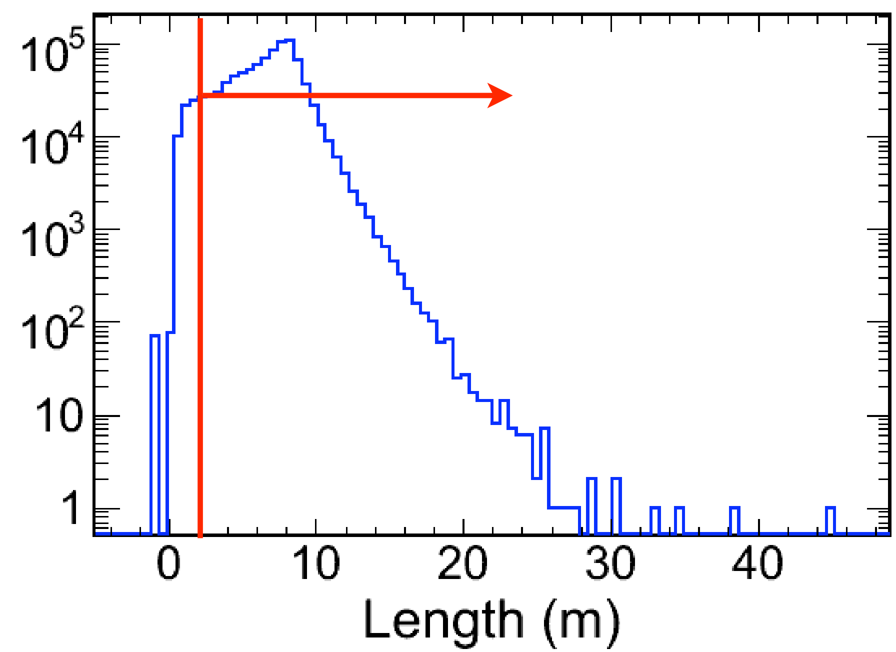

Neutrino-Induced Muon Analysis

FERMILAB-PUB-07-012-E, BNL-77481-2007-JA, hep-ex 0701045

Charge-Separated Atmospheric Neutrino-Induced Muons in the MINOS Far Detector

P. Adamson,[9,18] C. Andreopoulos,[23] K. E. Arms,[19] R. Armstrong,[12] D. J. Auty,[27] S. Avvakumov,[26] D. S. Ayres,[1] B. Baller,[9] B. Barish,[5] P. D. Barnes Jr.,[17] G. Barr,[21] W. L. Barrett,[31] E. Beall,[1,19,*] B. R. Becker,[19] A. Belias,[23] T. Bergfeld,[25,†] R. H. Bernstein,[9] D. Bhattacharya,[22] M. Bishai,[4] A. Blake,[6] B. Bock,[20] G. J. Bock,[9] J. Boehm,[10] D. J. Boehnlein,[9] D. Bogert,[9] P. M. Border,[19] C. Bower,[12] E. Buckley-Geer,[9] A. Cabrera,[21,‡] J. D. Chapman,[6] D. Cherdack,[30] S. Childress,[9] B. C. Choudhary,[9] J. H. Cobb,[21] A. J. Culling,[6] J. K. de Jong,[11] A. De Santo,[21,§] M. Dierckxsens,[4] M. V. Diwan,[4] M. Dorman,[18,23] D. Drakoulakos,[2] T. Durkin,[23] A. R. Erwin,[33] C. O. Escobar,[7] J. J. Evans,[21] E. Falk Harris,[27] G. J. Feldman,[10] T. H. Fields,[1] R. Ford,[9] M. V. Frohne,[3,¶] H. R. Gallagher,[30] G. A. Giurgiu,[1] A. Godley,[25] J. Gogos,[19] M. C. Goodman,[1] P. Gouffon,[24] R. Gran,[20] E. W. Grashorn,[19,20] N. Grossman,[9] K. Grzelak,[21] A. Habig,[20] D. Harris,[9] P. G. Harris,[27] J. Hartnell,[23] E. P. Hartouni,[17] R. Hatcher,[9] K. Heller,[19] A. Holin,[18] C. Howcroft,[5] J. Hylen,[9] D. Indurthy,[29] G. M. Irwin,[26] M. Ishitsuka,[12] D. E. Jaffe,[4] C. James,[9] L. Jenner,[18] D. Jensen,[9] T. Joffe-Minor,[1] T. Kafka,[30] H. J. Kang,[26] S. M. S. Kasahara,[19] M. S. Kim,[22] G. Koizumi,[9] S. Kopp,[29] M. Kordosky,[18] D. J. Koskinen,[18] S. K. Kotelnikov,[16] A. Kreymer,[9] S. Kumaratunga,[19] K. Lang,[29] A. Lebedev,[10] R. Lee,[10,**] J. Ling,[25] J. Liu,[29] P. J. Litchfield,[19] R. P. Litchfield,[21] P. Lucas,[9] W. A. Mann,[30] A. Marchionni,[9] A. D. Marino,[9] M. L. Marshak,[19] J. S. Marshall,[6] N. Mayer,[20] A. M. McGowan,[1,19] J. R. Meier,[19] G. I. Merzon,[16] M. D. Messier,[12] D. G. Michael,[5,††] R. H. Milburn,[30] J. L. Miller,[15,††] W. H. Miller,[19] S. R. Mishra,[25] A. Mislivec,[20] P. S. Miyagawa,[21] C. D. Moore,[9] J. Morfín,[9] L. Mualem,[5,19] S. Mufson,[12] S. Murgia,[26] J. Musser,[12] D. Naples,[22] J. K. Nelson,[32] H. B. Newman,[5] R. J. Nichol,[18] T. C. Nicholls,[23] J. P. Ochoa-Ricoux,[5] W. P. Oliver,[30] T. Osiecki,[29] R. Ospanov,[29] J. Paley,[12] V. Paolone,[22] A. Para,[9] T. Patzak,[8] Ž. Pavlović,[29] G. F. Pearce,[23] C. W. Peck,[5] E. A. Peterson,[19] D. A. Petyt,[19] H. Ping,[33] R. Piteira,[8] R. Pittam,[21] R. K. Plunkett,[9] D. Rahman,[19] R. A. Rameika,[9] T. M. Raufer,[21] B. Rebel,[9] J. Reichenbacher,[1] D. E. Reyna,[1] C. Rosenfeld,[25] H. A. Rubin,[11] K. Ruddick,[19] V. A. Ryabov,[16] R. Saakyan,[18] M. C. Sanchez,[10] N. Saoulidou,[9] J. Schneps,[30] P. Schreiner,[3] V. K. Semenov,[13] S.-M. Seun,[10] P. Shanahan,[9] W. Smart,[9] V. Smirnitsky,[14] C. Smith,[18,27] A. Sousa,[21,30] B. Speakman,[19] P. Stamoulis,[2] P.A. Symes,[27] N. Tagg,[30,21] R. L. Talaga,[1] E. Tetteh-Lartey,[28] J. Thomas,[18] J. Thompson,[22,††] M. A. Thomson,[6] J. L. Thron,[1,‡‡] G. Tinti,[21] I. Trostin,[14] V. A. Tsarev,[16] G. Tzanakos,[2] J. Urheim,[12] P. Vahle,[18] V. Verebryusov,[14] B. Viren,[4] C. P. Ward,[6] D. R. Ward,[6] M. Watabe,[28] A. Weber,[21,23] R. C. Webb,[28] A. Wehmann,[9] N. West,[21] C. White,[11] S. G. Wojcicki,[26] D. M. Wright,[17] Q. K. Wu,[25] T. Yang,[26] F. X. Yumiceva,[32] H. Zheng,[5] M. Zois,[2] and R. Zwaska[9]

(The MINOS Collaboration)

Neutrino-Induced Muon Selection

- Good timing resolution needed to separate neutrino-induced muons from cosmic ray muons
- Detector timing resolution ~ 2.3 ns
- Separate based on $1/\beta = c/v$ value for event
- $\Delta T/\Delta S$ used to determine $1/\beta$
    - ΔT is time difference between hit and vertex
    - ΔS is the distance between hit and vertex
- Downward-going have $1/\beta < 0$
- Upward-going have $1/\beta > 0$

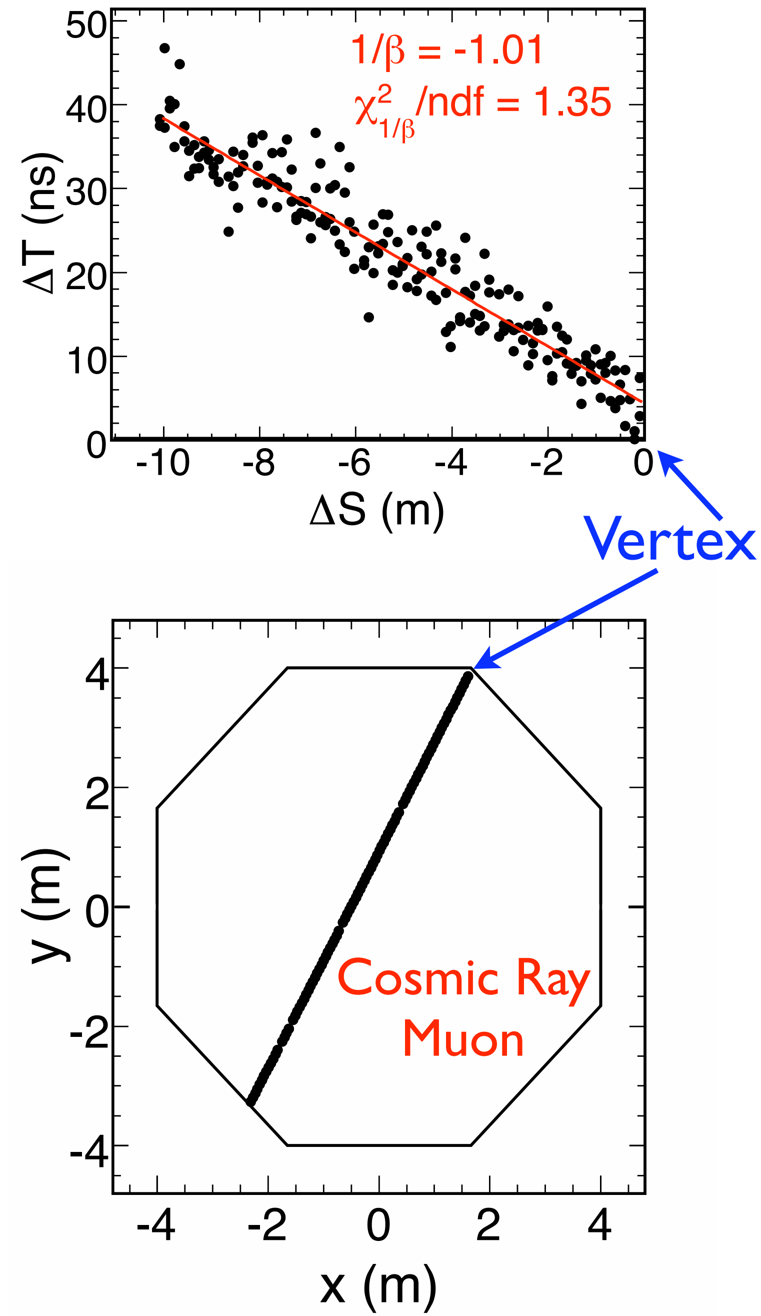

Neutrino-Induced Muon Selection

- Require fit for $1/\beta$ have $\chi^2/\mathrm{ndf} < 3$
- Upward-going events have $0.7 < 1/\beta < 1.3$
- At least half the strips in an events have signal on both ends
- Consistent direction between reconstruction and y vs time

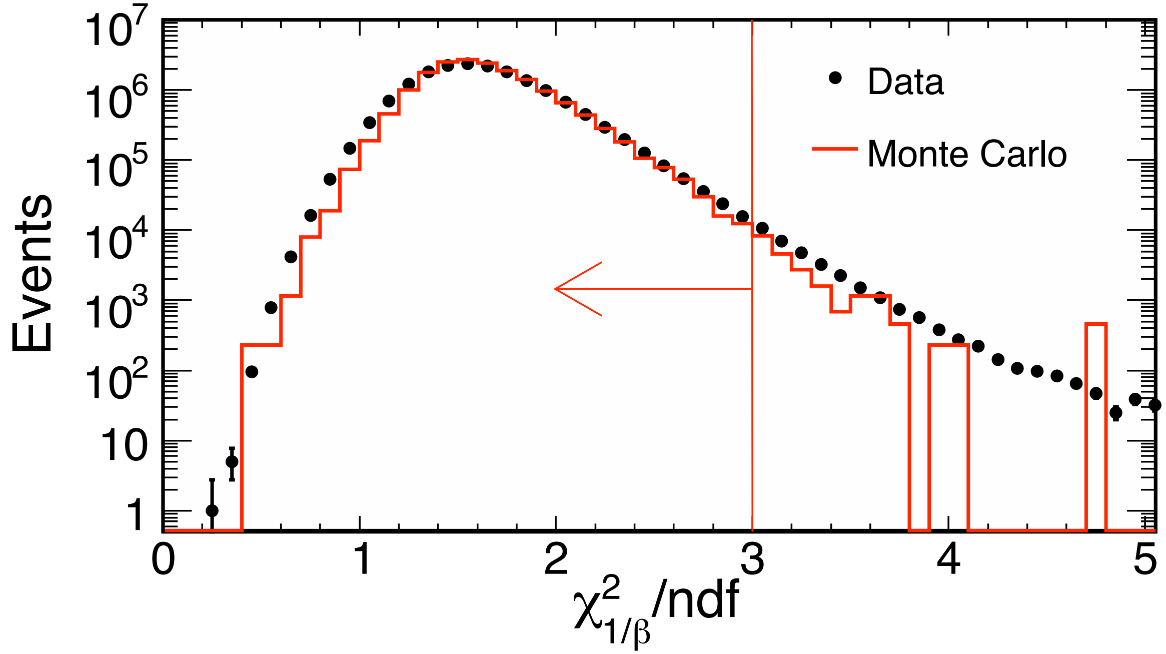

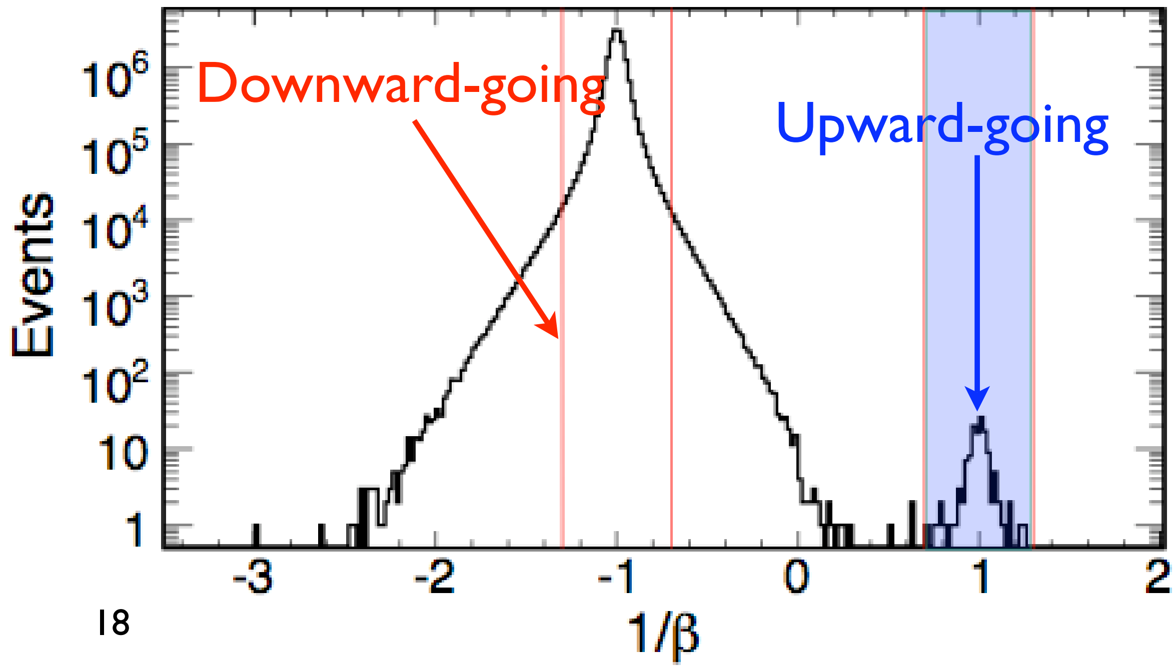

Neutrino-Induced Muon Selection

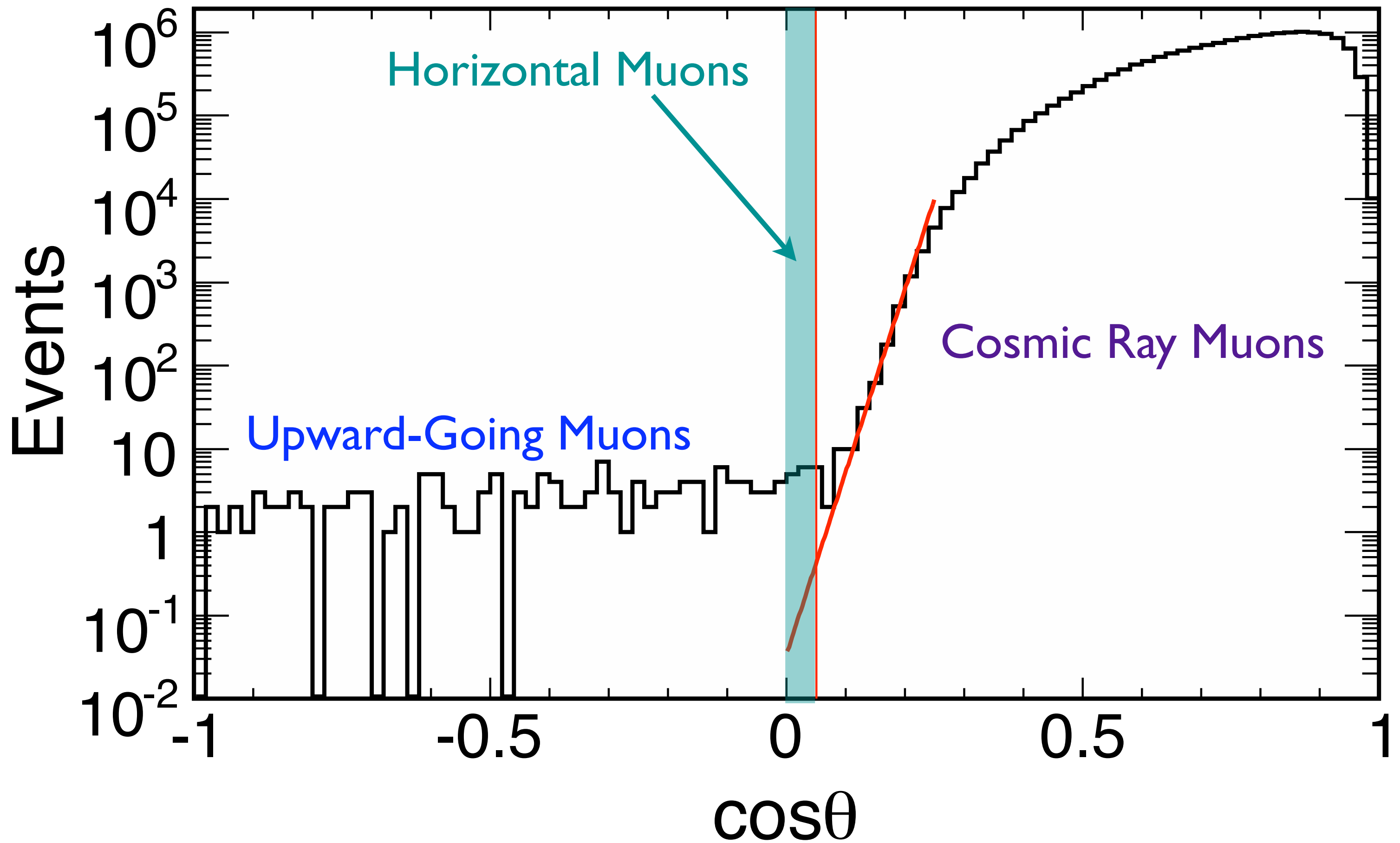

- Flat overburden allows search for neutrino-induced muons along horizon
- Horizontal events have new L/E range for neutrino-induced muon analysis
- Fit exponential to cosmic ray $\cos\theta$ distribution to determine cut
- Use events with $\cos\theta < 0.05$
- Also use fit to determine remaining background

Total Events Selected

Muon Type	Events	Background	
		Contained	Cosmic μ
Upward-going	130	4.2	0.0
Horizontal	10	0.1	0.3

- Total events selected is 140
- 130 upward-going
- 10 horizontal
- Backgrounds come from
  - Contained vertex events that pass our fiducial cuts
  - Cosmic ray muons that are energetic enough to penetrate the large overburden

Neutrino Disappearance with Neutrino-Induced Muons

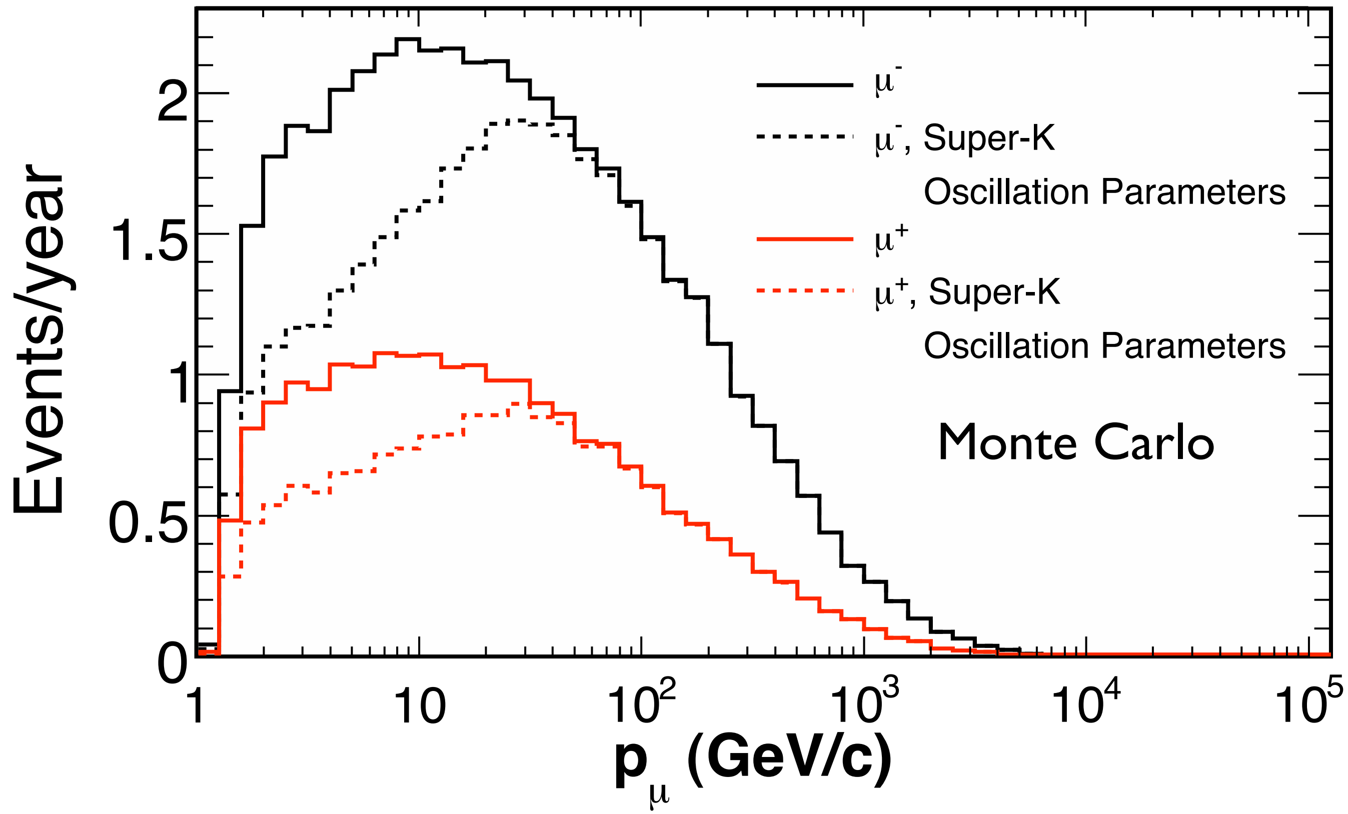

- Use neutrino-induced muons to look for oscillations
- Plot shows the expected number of events/year vs muon momentum
- Solid lines are without oscillations, dashed lines assuming Super-K best fit values
- Low momentum muons show evidence of disappearance

Parent Neutrino Energies for Neutrino-Induced Muons

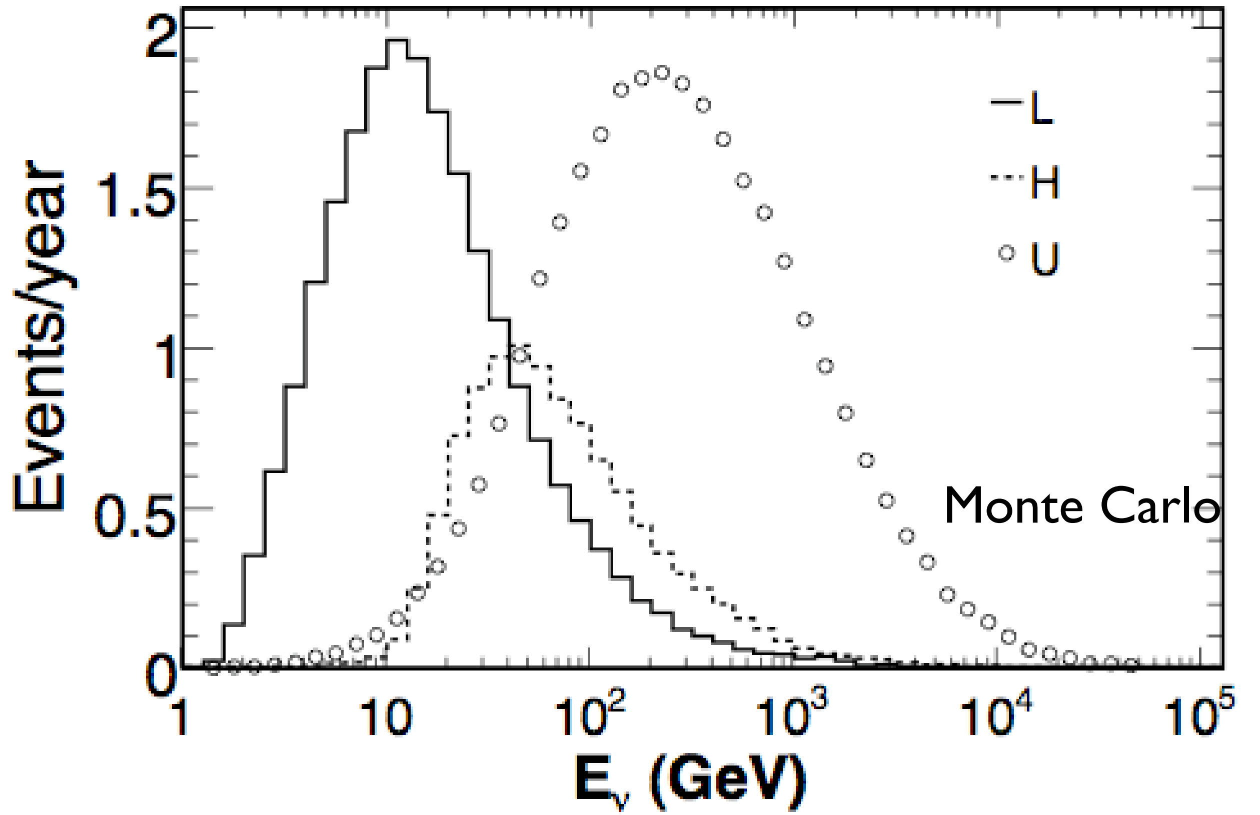

- Plot shows the distribution of parent neutrino energies for muons with
  - 1 < p < 10 GeV/c : Low
  - 10 < p < 100 GeV/c : High
  - Insufficient curvature information: Undetermined
- Expect low momentum muons to show most evidence of disappearance

Selecting Events with Good Momentum

- Use curvature in track to determine quality of charge and momentum determination
- Draw straight line between first and last point of track
- Find χ^2 for the fit
- Large curvature → good momentum determination
- Divide sample into 3 ranges on previous slide: L, H, and U
- Total events in each range and charge sign shown

p_{fit} (GeV)	Data	Bkgd	MC
	μ^-		
1 – 10 (L)	21	2.2	37.5
10 – 100 (H)	20	0.2	17.5
	μ^+		
1 – 10 (L)	16	1.3	19.3
10 – 100 (H)	13	0.2	8.6
	U		
unknown (U)	70	0.7	76.5

Evidence for Neutrino Disappearance

- Plot shows muon momentum distribution for events with good momentum determination
- See deficit at low momenta
- Find ratio of low to high and unknown events in data and Monte Carlo
- Double ratio should be unity if neutrino do not disappear
- See a 2σ difference from unity

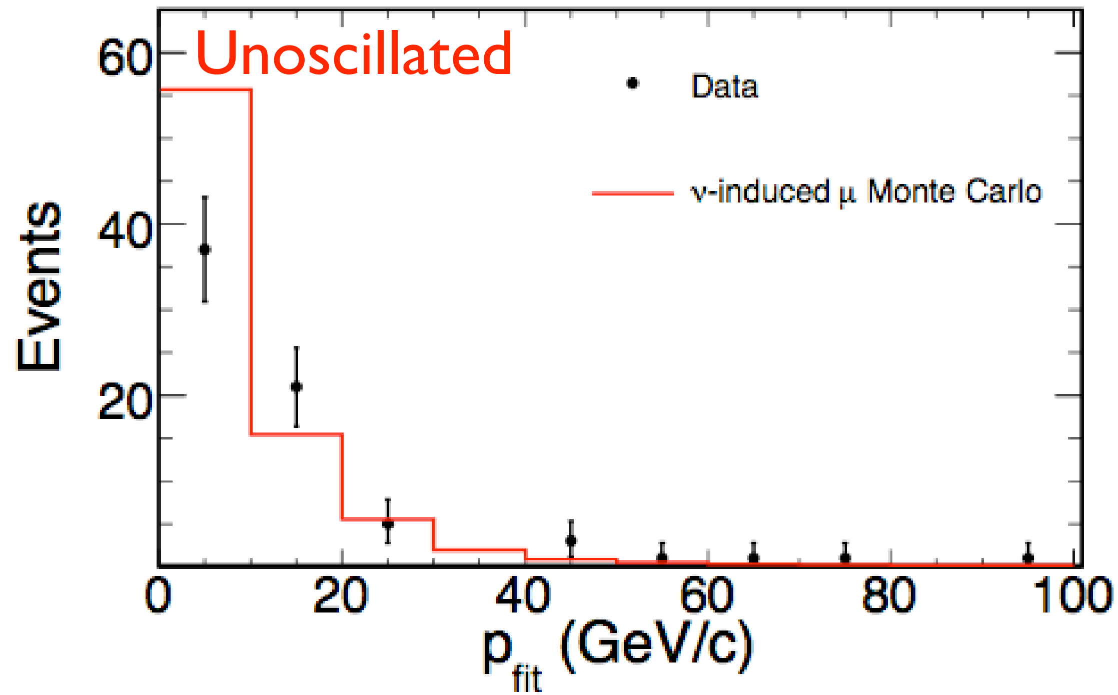

$$\mathcal{R} = \frac{R^{data}_{L/H+U}}{R^{MC}_{L/H+U}} = 0.65^{+0.15}_{-0.12}(\text{stat}) \pm 0.09(\text{syst})$$

Oscillation Analysis

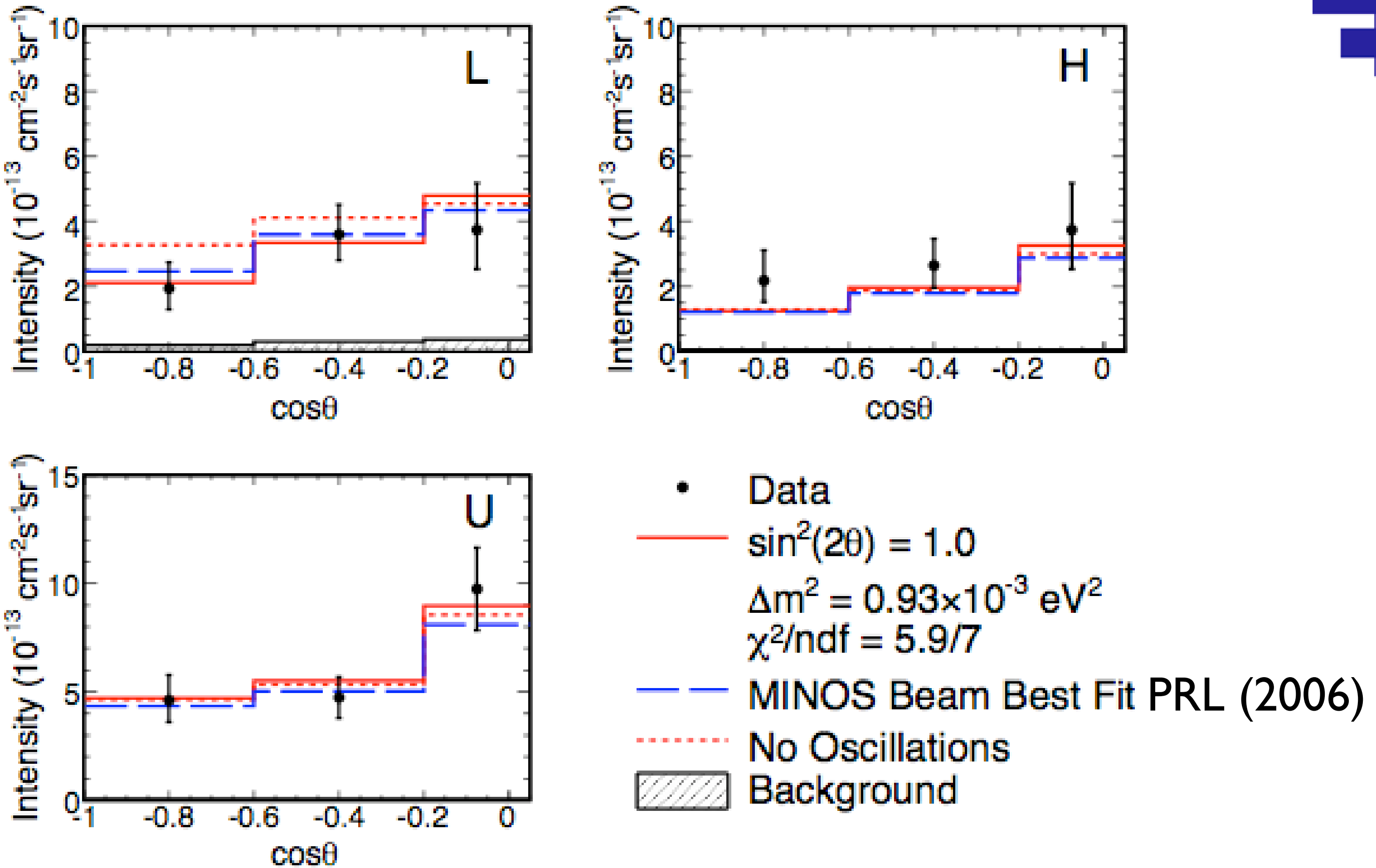

- Fit measured intensity in 3 bins of momentum and 3 bins of cosθ
- Oscillations would cause deficit of low momentum muons near nadir
- Include nuisance parameters to account for reconstruction and model systematics
- Best fit values: $\sin^2 2\theta = 1.0$, $\Delta m^2 = 0.93 \times 10^{-3}$ eV^2

Best Fit Contours

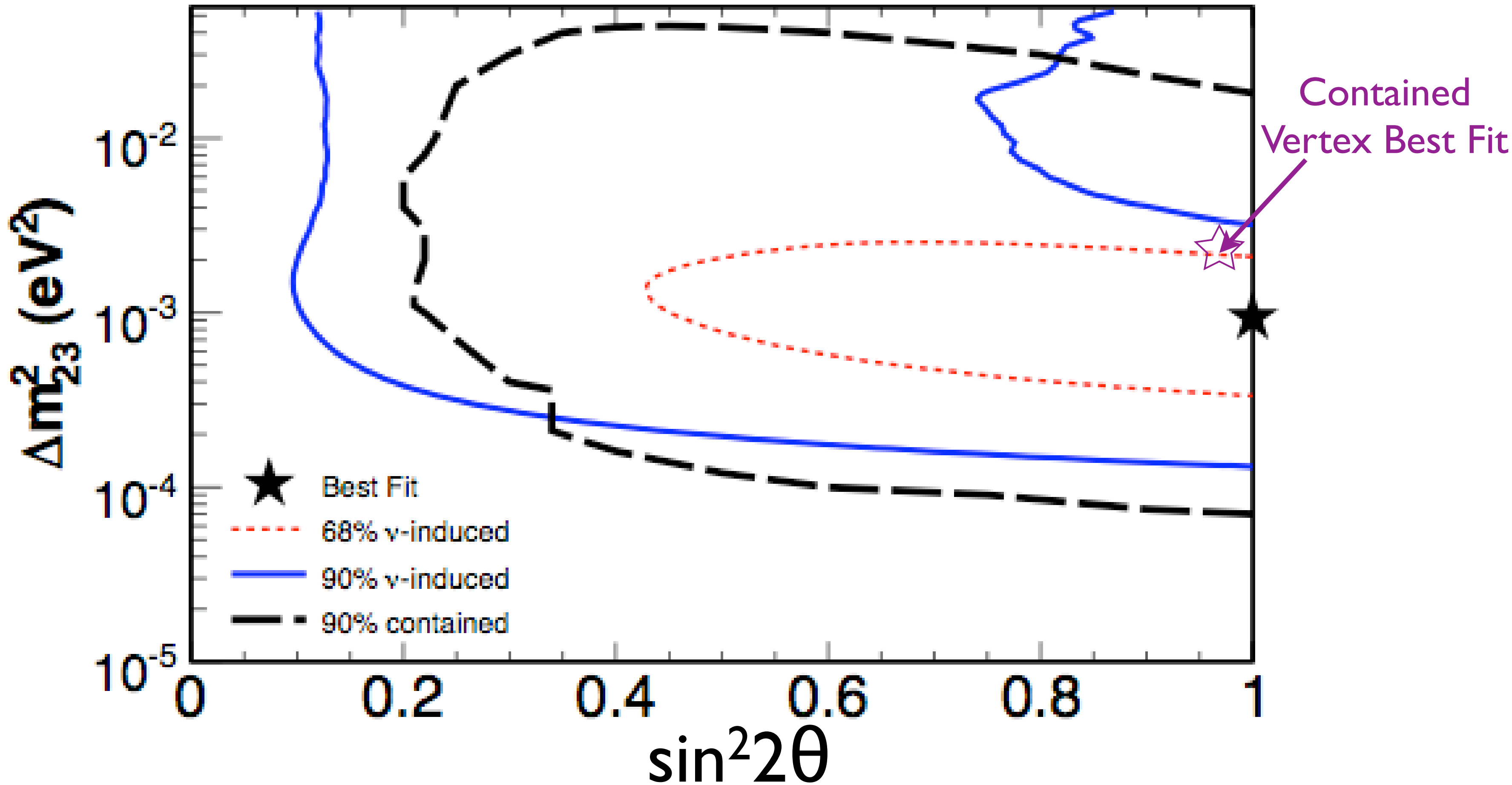

- Contours for 68% and 90% confidence levels shown
- Compare well with previous MINOS result using contained vertex atmospheric neutrinos - PRD 73:072002 (2006)

Test of CPT Conservation

- Use charge separated L and H events to test CPT conservation
- Expect ν_μ and $\bar{\nu}_\mu$ to disappear at the same rate if CPT conservation holds
- Compare ratio of total number of μ^- and μ^+ in data and Monte Carlo
- Ratio consistent with unity and CPT conservation

$$\hat{\mathcal{R}}_{CPT} = \frac{R^{data}_{\mu^-/\mu^+}}{R^{MC}_{\mu^-/\mu^+}} = 0.72^{+0.24}_{-0.18}(\text{stat})^{+0.08}_{-0.04}(\text{syst})$$

Recap of Neutrino-Induced Muon Results

- MINOS observes neutrino-induced muons from below and above the horizon
- Ratio of low momentum to sum of high momentum and unknown momentum shows neutrino disappearance
- Best fit for oscillation parameters at $\sin^2 2\theta = 1.0$, $\Delta m^2 = 0.93 \times 10^{-3}$ eV^2
- Observations of μ- and μ+ consistent with CPT conservation
- Future analysis will combine neutrino-induced muons and contained vertex events

Cosmic Ray Muon Charge Ratio Analysis

FERMILAB-PUB-07-134-E, BNL-78143-2007-JA, hep-ex 0705.3815

Measurement of the Atmospheric Muon Charge Ratio at TeV Energies with MINOS

P. Adamson,[1,2] C. Andreopoulos,[3] K. E. Arms,[4] R. Armstrong,[5] D. J. Auty,[6] S. Avvakumov,[7] D. S. Ayres,[8] B. Baller,[1] B. Barish,[9] P. D. Barnes Jr.,[10] G. Barr,[11] W. L. Barrett,[12] E. Beall,[8,4,*] B. R. Becker,[4] A. Belias,[3] T. Bergfeld,[13,†] R. H. Bernstein,[1] D. Bhattacharya,[14] M. Bishai,[15] A. Blake,[16] B. Bock,[17] G. J. Bock,[1] J. Boehm,[18] D. J. Boehnlein,[1] D. Bogert,[1] P. M. Border,[4] C. Bower,[5] E. Buckley-Geer,[1] C. Bungau,[6] A. Cabrera,[11,‡] J. D. Chapman,[16] D. Cherdack,[19] S. Childress,[1] B. C. Choudhary,[1,§] J. H. Cobb,[11] A. J. Culling,[16] J. K. de Jong,[20] A. De Santo,[11,¶] M. Dierckxsens,[15] M. V. Diwan,[15] M. Dorman,[2,3] D. Drakoulakos,[21] T. Durkin,[3] A. R. Erwin,[22] C. O. Escobar,[23] J. J. Evans,[11] E. Falk Harris,[6] G. J. Feldman,[18] T. H. Fields,[8] R. Ford,[1] M. V. Frohne,[24,**] H. R. Gallagher,[19] G. A. Giurgiu,[8] A. Godley,[13] J. Gogos,[4] M. C. Goodman,[8] P. Gouffon,[25] R. Gran,[17] E. W. Grashorn,[4,17] N. Grossman,[1] K. Grzelak,[11] A. Habig,[17] D. Harris,[1] P. G. Harris,[6] J. Hartnell,[3] E. P. Hartouni,[10] R. Hatcher,[1] K. Heller,[4] A. Holin,[2] C. Howcroft,[9] J. Hylen,[1] D. Indurthy,[26] G. M. Irwin,[7] M. Ishitsuka,[5] D. E. Jaffe,[15] C. James,[1] L. Jenner,[2] D. Jensen,[1] T. Joffe-Minor,[8] T. Kafka,[19] H. J. Kang,[7] S. M. S. Kasahara,[4] M. S. Kim,[14] G. Koizumi,[1] S. Kopp,[26] M. Kordosky,[2] D. J. Koskinen,[2] S. K. Kotelnikov,[27] A. Kreymer,[1] S. Kumaratunga,[4] K. Lang,[26] A. Lebedev,[18] R. Lee,[18,††] J. Ling,[13] J. Liu,[26] P. J. Litchfield,[4] R. P. Litchfield,[11] P. Lucas,[1] W. A. Mann,[19] A. Marchionni,[1] A. D. Marino,[1] M. L. Marshak,[4] J. S. Marshall,[16] N. Mayer,[17] A. M. McGowan,[8,4] J. R. Meier,[4] G. I. Merzon,[27] M. D. Messier,[5] D. G. Michael,[9,‡‡] R. H. Milburn,[19] J. L. Miller,[28,‡‡] W. H. Miller,[4] S. R. Mishra,[13] A. Mislivec,[17] P. S. Miyagawa,[11] C. D. Moore,[1] J. Morfín,[1] L. Mualem,[4] S. Mufson,[5] S. Murgia,[7] J. Musser,[5] D. Naples,[14] J. K. Nelson,[29] H. B. Newman,[9] R. J. Nichol,[2] T. C. Nicholls,[3] J. P. Ochoa-Ricoux,[9] W. P. Oliver,[19] T. Osiecki,[26] R. Ospanov,[26] J. Paley,[5] V. Paolone,[14] A. Para,[1] T. Patzak,[30] Ž. Pavlović,[26] G. F. Pearce,[3] C. W. Peck,[9] E. A. Peterson,[4] D. A. Petyt,[4] H. Ping,[22] R. Piteira,[30] R. Pittam,[11] R. K. Plunkett,[1] D. Rahman,[4] R. A. Rameika,[1] T. M. Raufer,[11] B. Rebel,[1] J. Reichenbacher,[8] D. E. Reyna,[8] C. Rosenfeld,[13] H. A. Rubin,[20] K. Ruddick,[4] V. A. Ryabov,[27] R. Saakyan,[2] M. C. Sanchez,[18] N. Saoulidou,[1] J. Schneps,[19] P. Schreiner,[24] V. K. Semenov,[31] S.-M. Seun,[18] P. Shanahan,[1] W. Smart,[1] V. Smirnitsky,[32] C. Smith,[2,6] A. Sousa,[11,19] B. Speakman,[4] P. Stamoulis,[21] P.A. Symes,[6] N. Tagg,[19,11] R. L. Talaga,[8] E. Tetteh-Lartey,[33] J. Thomas,[2] J. Thompson,[14,‡‡] M. A. Thomson,[16] J. L. Thron,[8,§§] G. Tinti,[11] I. Trostin,[32] V. A. Tsarev,[27] G. Tzanakos,[21] J. Urheim,[5] P. Vahle,[2] C. Velissaris,[22] V. Verebryusov,[32] B. Viren,[15] C. P. Ward,[16] D. R. Ward,[16] M. Watabe,[33] A. Weber,[11,3] R. C. Webb,[33] A. Wehmann,[1] N. West,[11] C. White,[20] S. G. Wojcicki,[7] D. M. Wright,[10] Q. K. Wu,[13] T. Yang,[7] F. X. Yumiceva,[29] H. Zheng,[9] M. Zois,[21] and R. Zwaska[1]
(The MINOS Collaboration)

Cosmic Ray Charge Ratio

- Cosmic ray primaries have positive charge
- More positive pions and kaons produced than negative
- Charge ratio of muons will be > 1
- Goal of analysis is to measure ratio $R = \frac{N_{\mu^+}}{N_{\mu^-}}$

- Charge ratio important for modeling cosmic ray interactions
  - Increasing importance of kaons - increased ratio with increasing energy
  - Larger role from heavy elements - decreased ratio with increasing energy
  - Increase charm production - decreased ratio with increasing energy
- Charge ratio constrains atmospheric neutrino flux models and ratio of $\nu_\mu / \bar{\nu}_\mu$

Data Sets

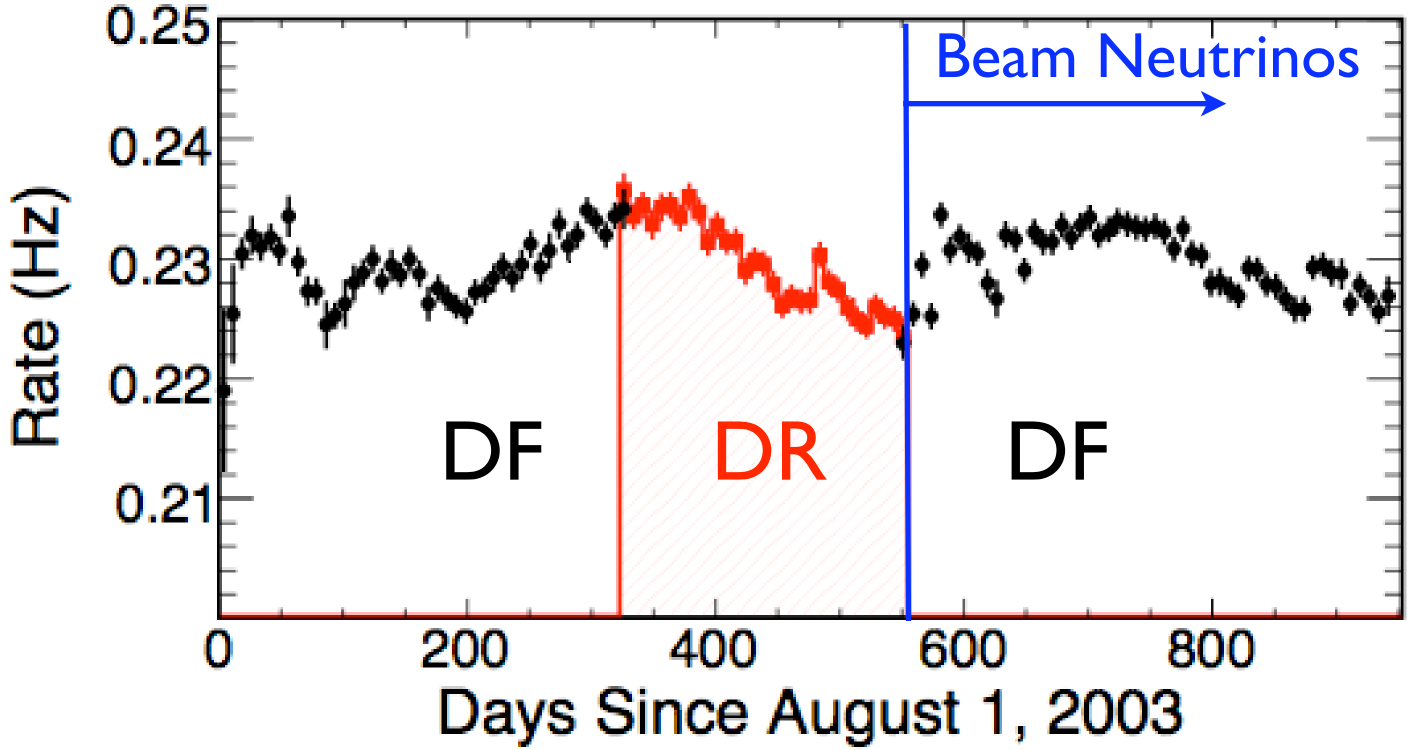

- Data taken in 2 configurations of magnetic field
- Forward running focused μ^- from the south (DF) - 609.82 live days
- Reverse running focused μ^+ from the south (DR) - 201.75 live days
- Plot shows daily rate, fluctuations consistent with seasonal effects

Charge Sign Analysis Event Selection

- Cosmic rays have different energies and event characteristics than neutrino-induced muons
- Use different charge sign identification cuts than neutrino-induced muon analysis
- Good track fitting cut - $(q/p)/\sigma_{q/p} > 2.2$
- Charge ratio goes to unity as track fitting gets worse - random charge ID
- Additional cuts also needed to remove systematics

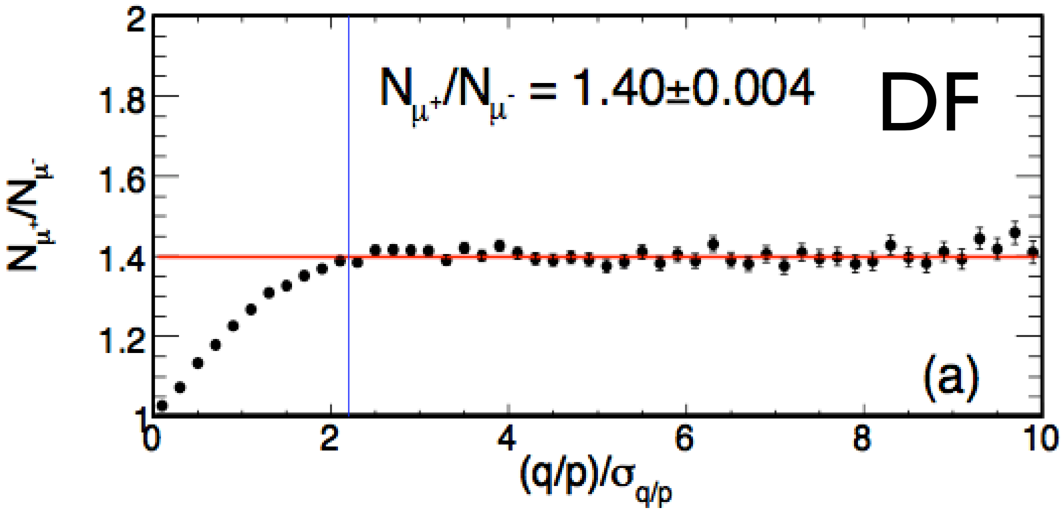

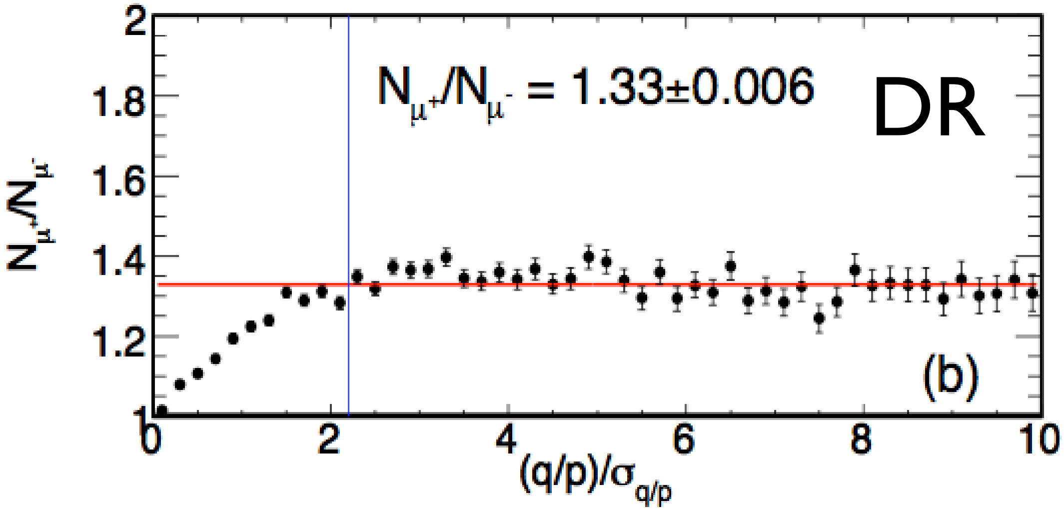

Determining Cosmic Ray Muon Charge

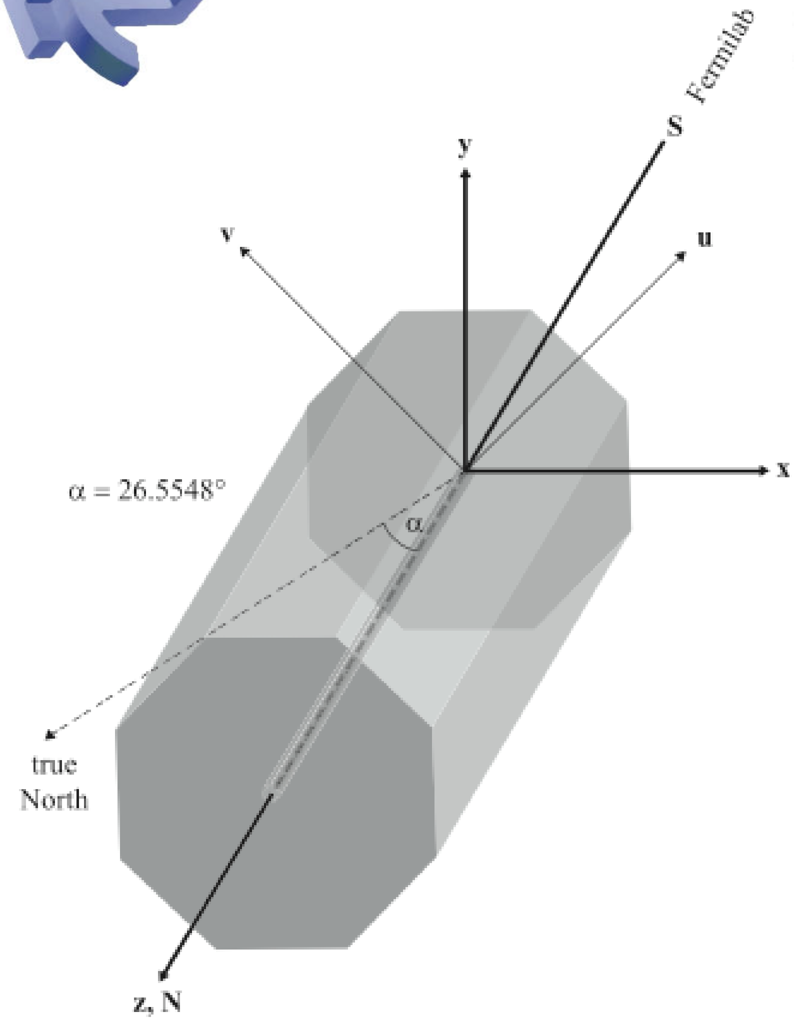

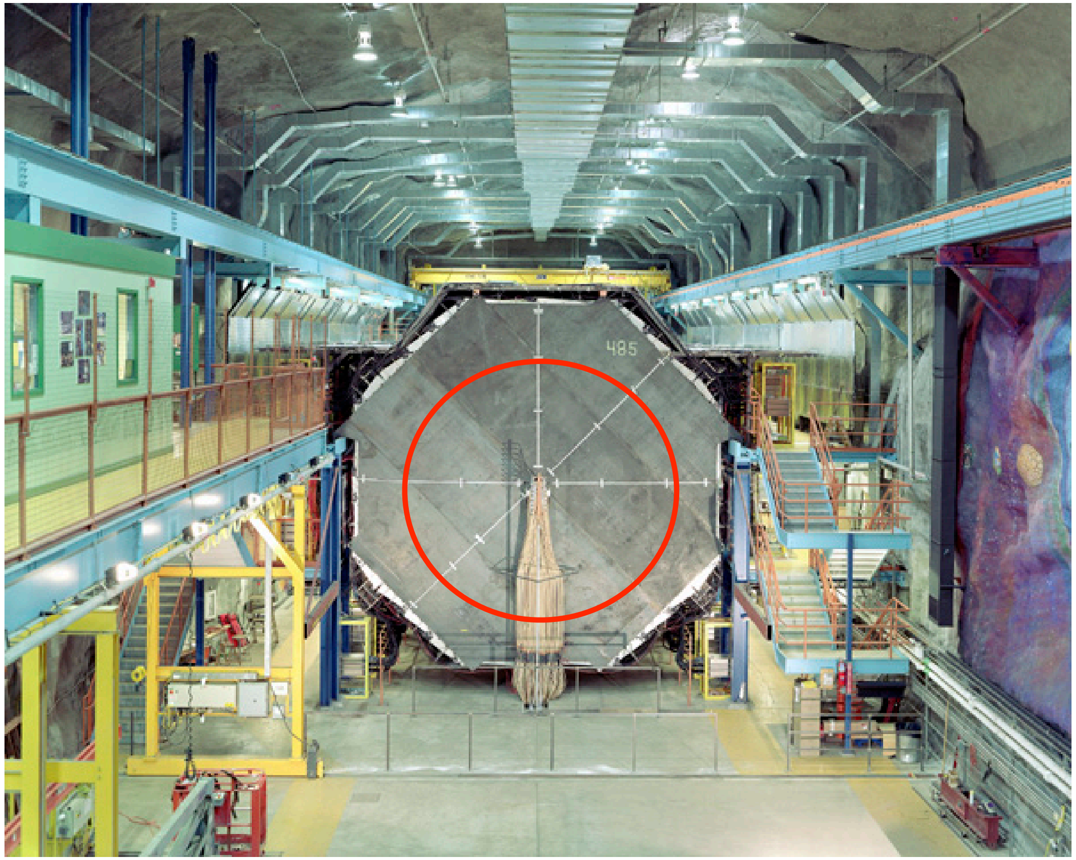

- Field and alignment are best known near center of detector
- Field also strongest near coil
- Expect muons crossing many planes in this region to have better fit than those crossing the outer regions

Charge Identification Selection

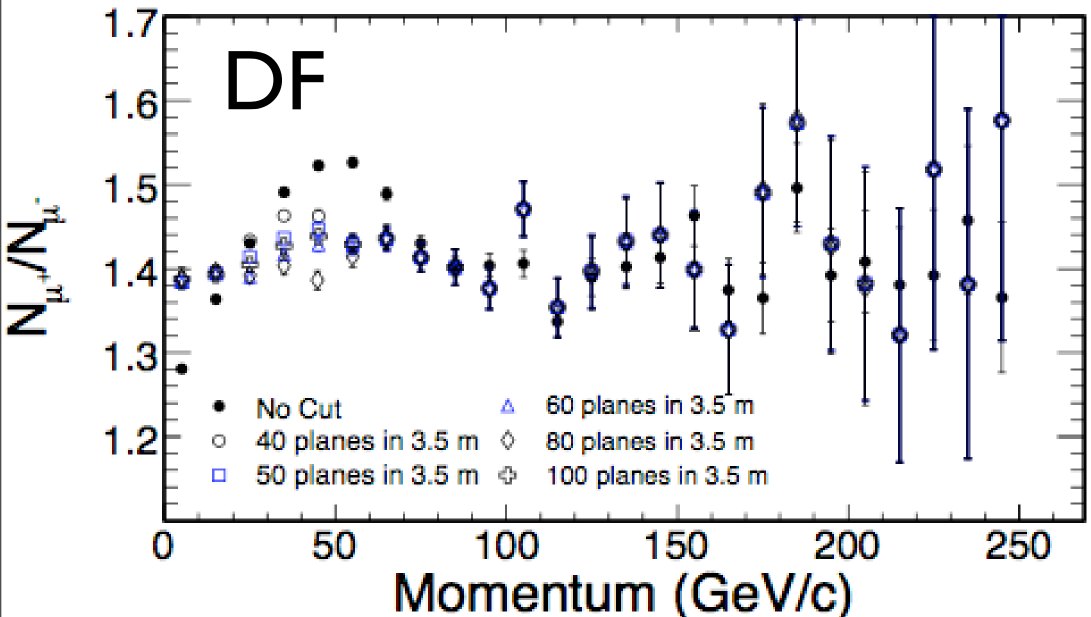

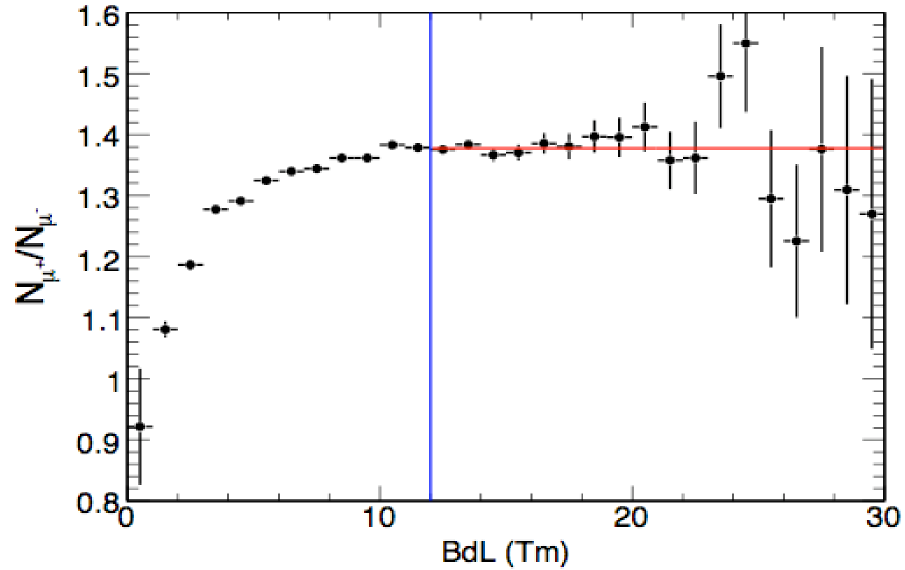

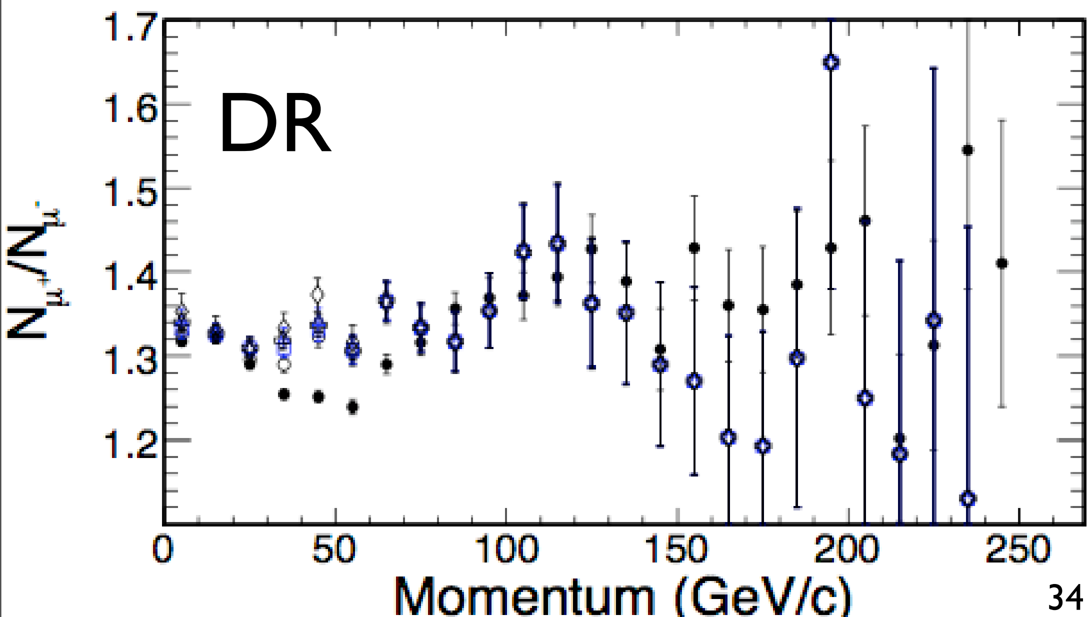

- Minimum information cut (MIC) - muon within 3.5 m of coil for at least 60 planes
- OR BdL - product of magnetic field and distance traveled by muon > 12 Tm
- Underground ratio is average of these

Minimizing Systematics

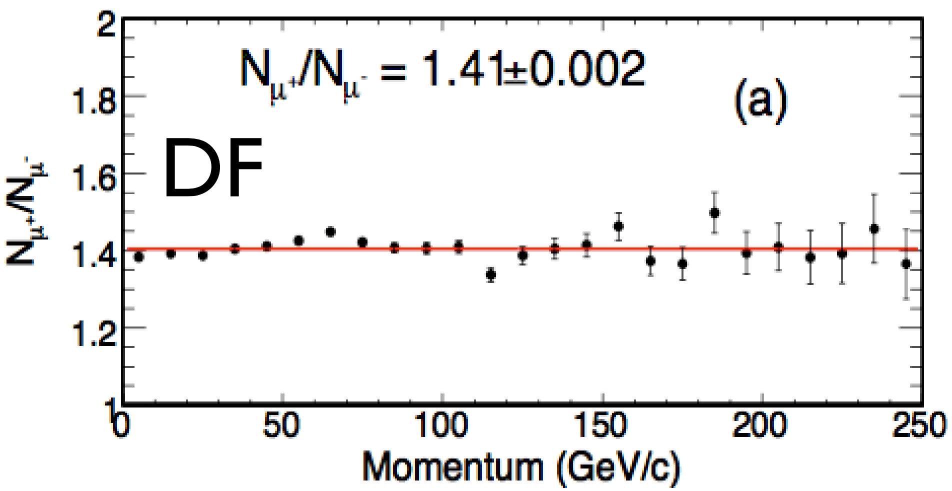

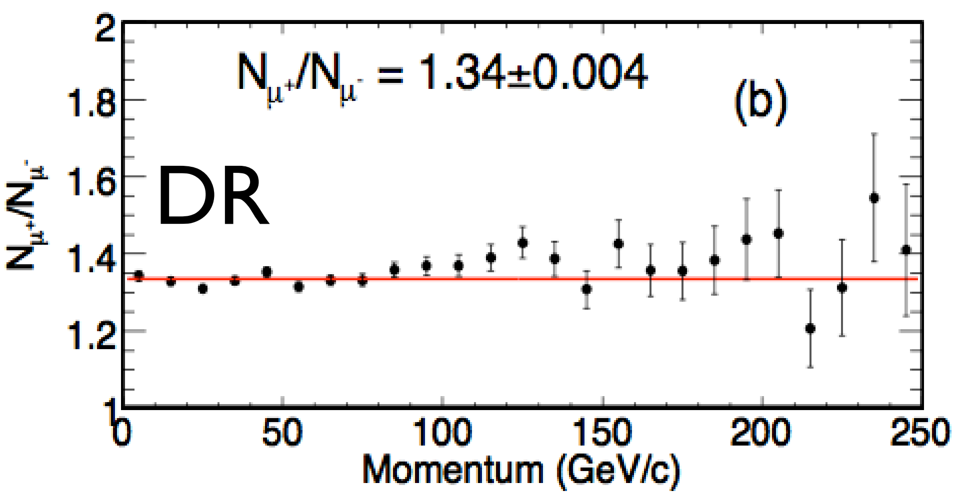

- Offset remains in charge ratio for forward and reverse data sets
- Acceptance major component of offset
- Use geometric mean of ratios to cancel acceptance effects

$$r_a = (N_{\mu^+}/t)_{DF}/(N_{\mu^-}/t)_{DR}$$

$$r_b = (N_{\mu^+}/t)_{DR}/(N_{\mu^-}/t)_{DF}$$

$$r = [r_a \times r_b]^{1/2} = [(N_{\mu^+}/N_{\mu^-})_{DF} \times (N_{\mu^+}/N_{\mu^-})_{DR}]^{1/2}$$

- Can cancel live time related systematics by using equal sized samples in geometric mean

Underground Charge Ratio

- Consider 3 sources of systematics
  - Incomplete cancelation in combination of DF and DR sets
  - Changes over time in detector
  - Remaining random charge ID
- Plot shows ratio for MIC analysis
- Final underground ratio is below

Source	$(\sigma_{syst})_i$
1. Combining Forward/Reverse	$\pm$ 0.009
2. Sliding Window	$\pm$ 0.005
3. Randomization	+0.007
$\sigma_{syst} = \sqrt{\sum_i (\sigma_{syst})_i^2}$	(+0.012, -0.010)

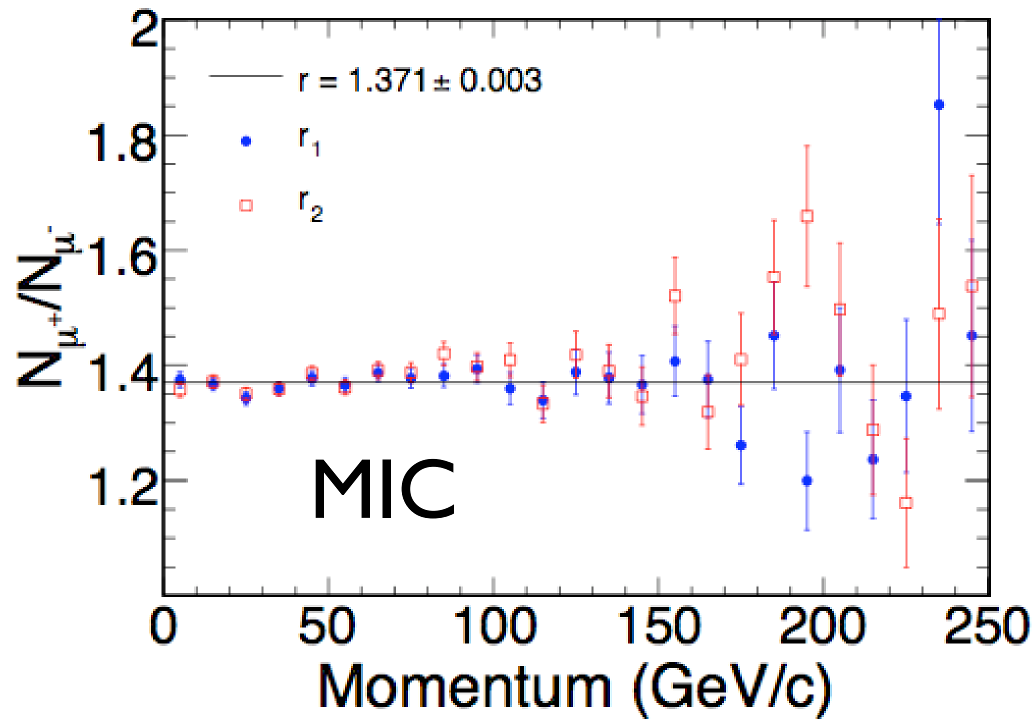

$$r = 1.374 \pm 0.004\,(\text{stat.})^{+0.012}_{-0.010}\,(\text{sys.})$$

Vertical Muon Intensity

$$(I_\mu)_j = \frac{1}{T}\frac{mN_j}{(\epsilon_j A_j \Delta\Omega/\cos\theta_j)}$$

Multiplicity Correction (m)

Number of muons observed in solid angle bin (N_j)

Correction to vertical for solid angle bin ($\cos\theta_j$)

Live Time (T)

Efficiency (ϵ_j)

Projected Area (A_j)

Solid Angle ($\Delta\Omega$)

- Sort single muons into solid angle bins
- Compute intensity for each bin
- Match value bin by bin to Crouch curve to get slant depth
- Slant depth is column of rock between detector and surface

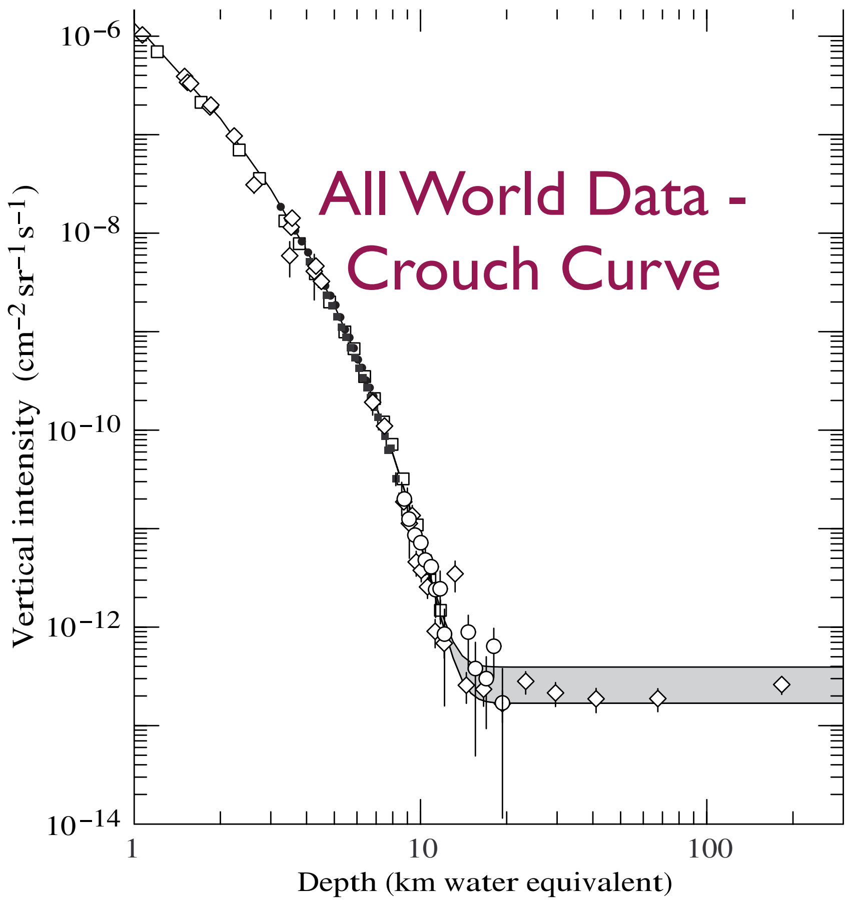

Measured Vertical Muon Intensity

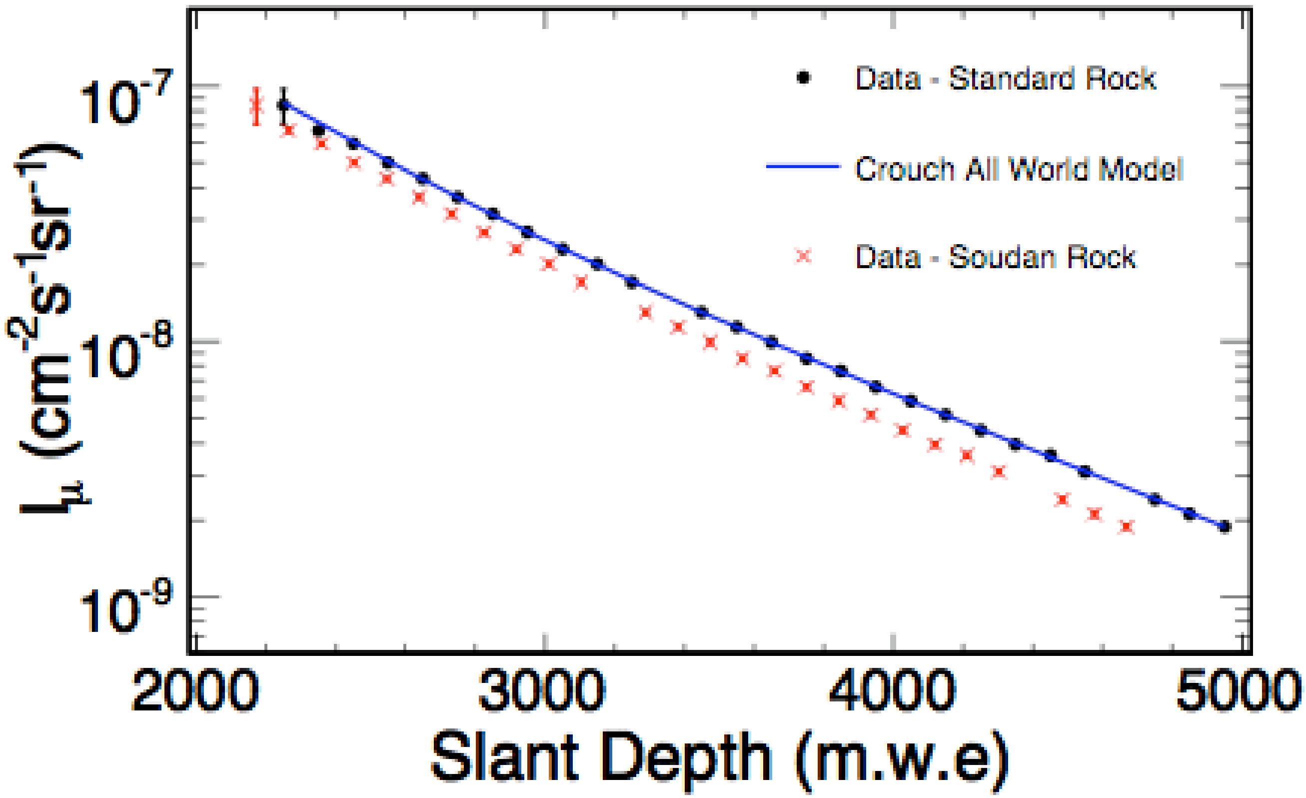

- Method produces map of slant depths around detector
- 1 m.w.e = 100 g/cm^2
- This plot and the remaining plots are made from the MIC analysis

Correct to Soudan Rock

- Ely greenstone surrounding MINOS is denser than standard rock
- Convert slant depth map to MINOS rock using

$$X_M = \frac{1}{b_M} \ln\left[1 + \left(\frac{a_s}{b_s}\right)\left(\frac{b_M}{a_M}\right)\left(e^{b_s X_s} - 1\right)\right]$$

$$b_M = b_s \langle \frac{Z_M^2}{A_M} \rangle \langle \frac{Z_s^2}{A_s} \rangle^{-1}$$

$$a_M = a_s \langle \frac{Z_M}{A_M} \rangle \langle \frac{Z_s}{A_s} \rangle^{-1}$$

- Values for constants given in tables

	$\langle Z/A \rangle$	$\langle Z^2/A \rangle$
Standard Rock	0.5	5.5
Soudan Rock	0.5	6.1

Radiative Energy Loss Factor

Collisional Energy Loss Factor

E_μ GeV	R km.w.e.	a MeV g^{-1} cm^2	$b_{\rm brems}$	$b_{\rm pair}$ 10^{-6} g^{-1} cm^2	$b_{\rm nucl}$	$\sum b_i$
10	0.05	2.17	0.70	0.70	0.50	1.90
100	0.41	2.44	1.10	1.53	0.41	3.04
1000	2.45	2.68	1.44	2.07	0.41	3.92
10000	6.09	2.93	1.62	2.27	0.46	4.35

Charge Ratio vs Slant Depth

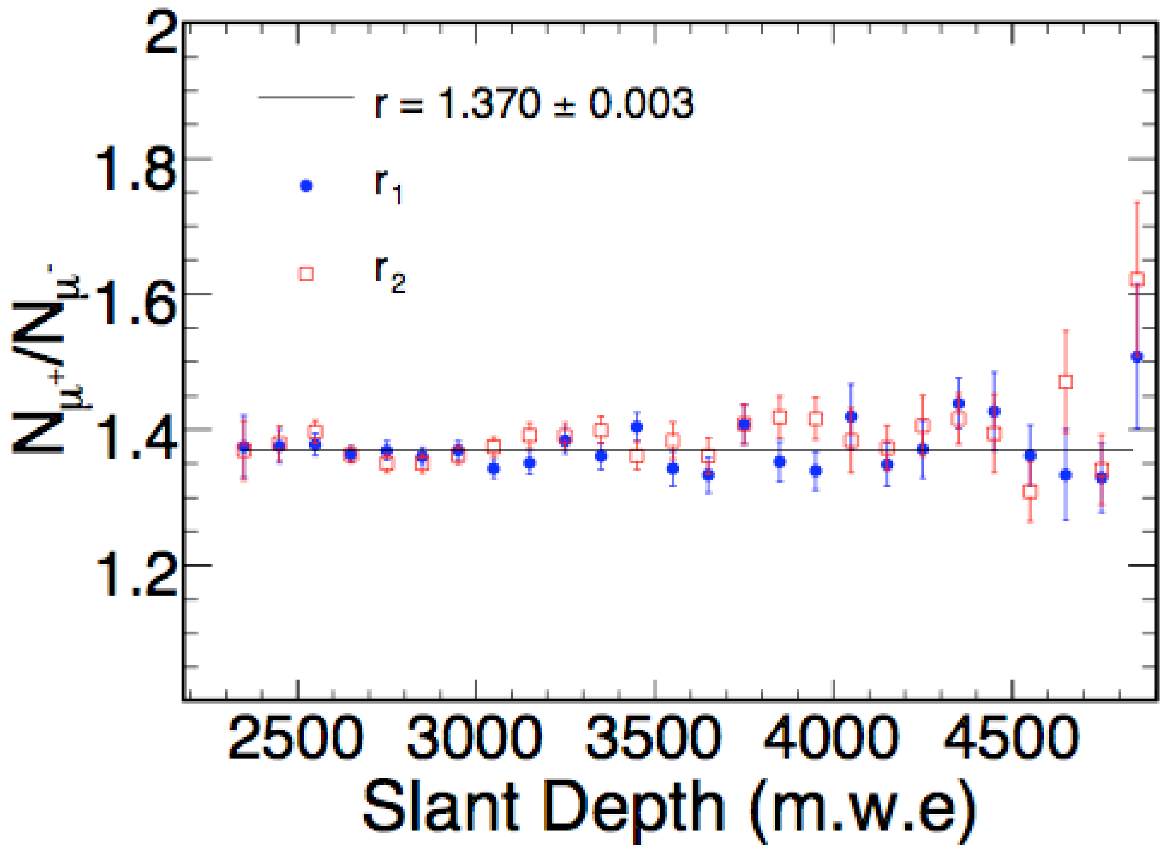

- Charge ratio as a function of Soudan rock
- Charge ratio independent of slant depth

Determining Surface Energies

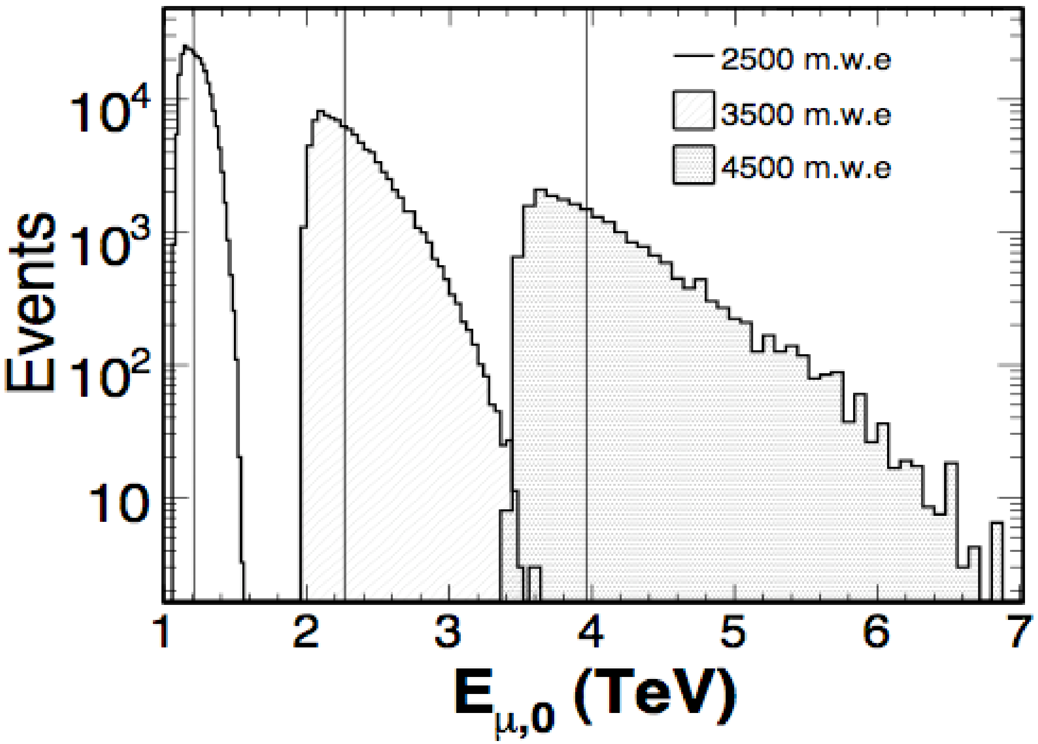

- Muons lose energy according to

$$-\frac{\mathrm{d}E_\mu}{\mathrm{d}X} = a(E_\mu) + b(E_\mu)E_\mu$$

- At the surface the muon energy is

$$E_{\mu,0} = (E_\mu + a/b)e^{bX} - a/b$$

- Each muon is projected back to the surface using above equations
- Distributions of surface energies for slant depth bins of size 100 mwe shown
- Higher surface energies needed to penetrate larger columns of rock

Charge Ratio At Surface

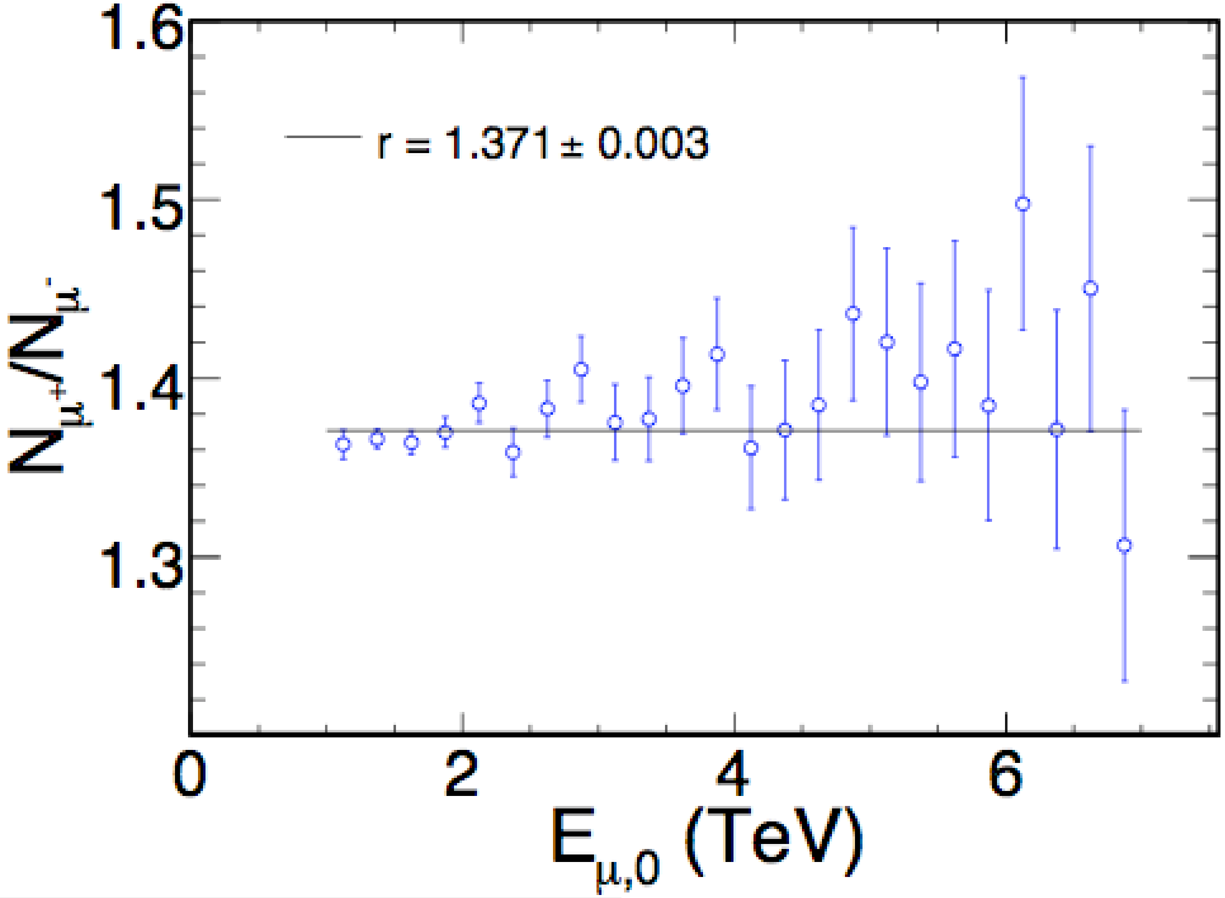

- Charge ratio at surface shown in plot - 1.371 ± 0.003(stat) + 0.012 - 0.010(sys)
- L3+C measured charge ratio ~ 1.285 ± 0.003(stat) ± 0.019(sys)
- Significant increase over previous measurements

Increase in Charge Ratio

- L3+C measurement for muon energies < 300 GeV
- Expect charge ratio to increase with energy as kaon contribution increases
- K^+/K^- ratio is larger than π^+/π^-
- As energy increases the kaon contribution becomes more important in the muon charge ratio
- Use qualitative model to explain increasing charge ratio

Fraction of π decays making μ^+

Fraction of K decays making μ^+

$$\frac{N_{\mu^+}}{N_{\mu^-}} = \left[\frac{f_{\pi^+}}{1+\frac{1.1E_{\mu^+}\cos\theta}{115\ \text{GeV}}} + \frac{0.054 f_{K^+}}{1+\frac{1.1E_{\mu^+}\cos\theta}{850\ \text{GeV}}}\right] \Bigg/ \left[\frac{(1-f_{\pi^+})}{1+\frac{1.1E_{\mu^-}\cos\theta}{115\ \text{GeV}}} + \frac{0.054(1-f_{K^+})}{1+\frac{1.1E_{\mu^-}\cos\theta}{850\ \text{GeV}}}\right]$$

πK Model

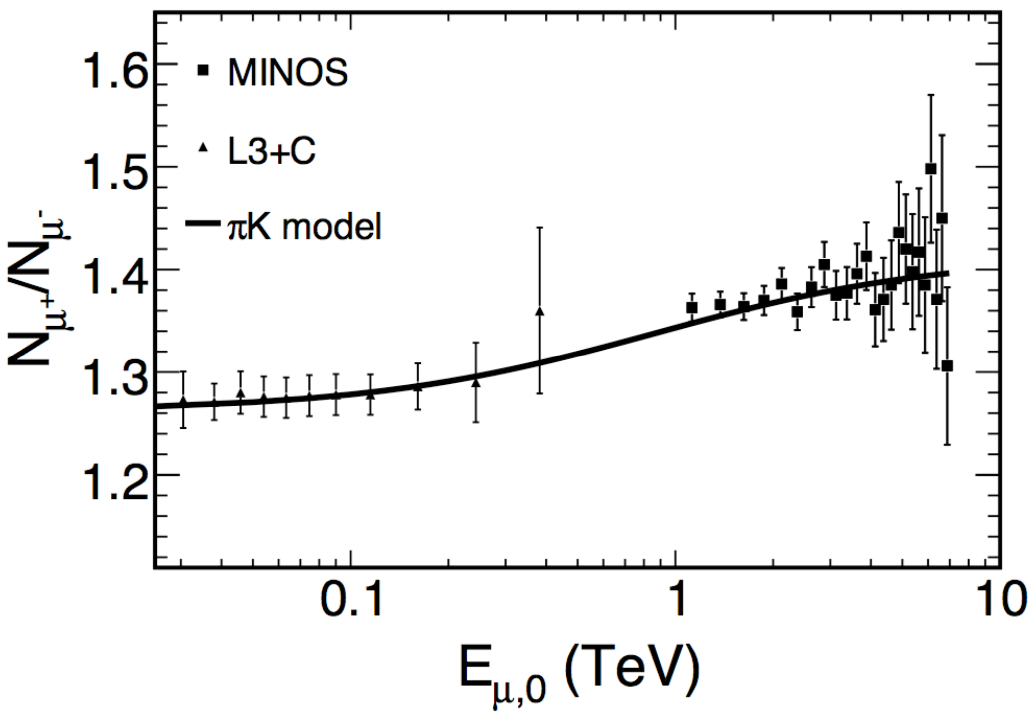

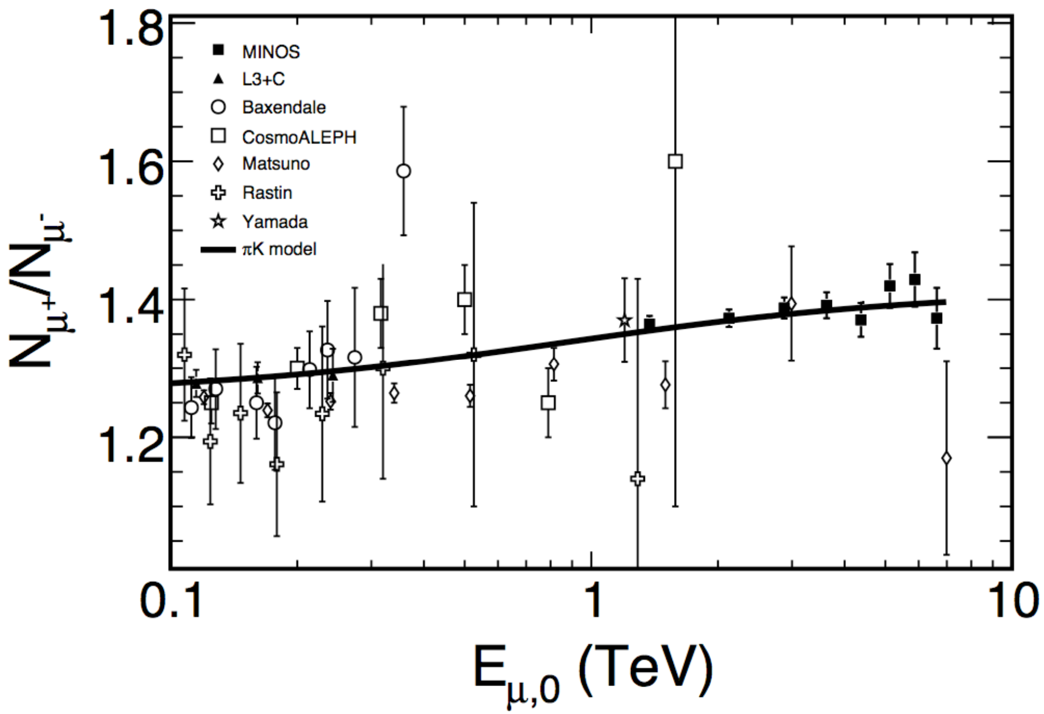

- MINOS and L3+C data shown in plot
- πK model describes increase of charge ratio as a result of kaon contribution becoming more important
- Best fit values - $f_{\pi+} = 0.55$, $f_{K+} = 0.67$

Conclusions

- MINOS sees increased charge ratio
- Qualitative πK model explains increase in charge ratio
- Increase due to kaons becoming more important in ratio
- Model is consistent with available data
- Preliminary analysis of Near Detector confirms rise in charge ratio